Addis Ababa University

Addis Ababa Institute of Technology

School of Electrical and Computer Engineering

Modeling and Analysis of Regenerative Braking of an Induction Motor

---

By: Lidia Habtamu

A Thesis Submitted To School of Electrical and Computer Engineering of Addis Ababa University in Partial Fulfillment of the Requirement for Masters Degree in Control Engineering

Advisor: Dr Mengesha Mamo

April, 2017
Addis Ababa, Ethiopia

Addis Ababa University

Addis Ababa Institute of Technology

School of Electrical and Computer Engineering

A Thesis Submitted To School of Electrical and Computer Engineering of Addis Ababa University in Partial Fulfillment of the Requirement for Masters Degree in Control Engineering

By: Lidia Habtamu

Approval by Board of Examiners

Approved by:

1.	----------	----------	----------
	Advisor	Signature	Date
2.	----------	----------	----------
	Chairman Dep.'s Graduate Committee	Signature	Date
3.	----------	----------	----------
	Chairman Faculty's Graduate Committee	Signature	Date
4.	----------	----------	----------
	Dean Graduate School	Signature	Date

DECLARATION

I, the undersigned, declare that this thesis is my original work and has never been presented in this or any other university and that all the source materials used for the thesis have been fully acknowledged.

Name: Lidia Habtamu (B.Sc.)

Signature: _____

Place: Addis Ababa

Date of submission: _____

This thesis has been submitted for examination with my approval as a university advisor.

Name: Dr Mengesha Mamo (PHD)

Signature: _____

Date: _____

Acknowledgement

I would like to extend my sincere gratitude to my advisor Dr Mengesha Mamo for his unreserved guidance and comments from the stage of the research proposal up to thesis write-up.

My heartfelt thanks go to Addis Ababa University for arranging a financial support without which this research would not have materialized. I would like to express my appreciation to all who helped me with the kit.

Finally, I would like to thank staffs of the School of Electrical and Computer engineering control lab especially Mr Teshome Hambessa for his invaluable support to this thesis work.

Abstract

Due to the increase in demand of energy, new technologies have evolved to improve energy efficiency like regenerative braking. In this thesis, the energy storage device, battery, with converters and IM are used to analyze regenerative braking. Using only battery and IM is easy in control but adding converters result in a better performance. The analysis is performed using vector control method and MATLAB SIMULINK as simulation tool. The results show that the desired energy saving (around 500Watt) can be obtained during regenerative braking. An experimental analysis using Texas instruments Digital Signal Processor C2000 F28035 was performed. The torque producing current component, the dc bus voltage and decelerating speed has been analyzed during regenerative braking mode. From the experiment the torque producing current component becomes negative when regeneration starts. To analyze the time needed for the motor to stop two experiments have done. The result demonstrates that the braking time during regenerative braking is shorter than that of free fall. During regenerative braking the dc bus voltage was supposed to increase however due to the small inertia of the motor the voltage increase was not observed. But by adding additional disk to IM, the inertia of the motor was increased and energy regeneration was observed.

Keywords: Regenerative braking, Energy regeneration, Vector control, Sensorless

Table of Content

Acknowledgement ----------I

Abstract----------II

Table of Content----------III

List of Tables----------V

List of Figures----------VI

List of Abbreviations----------VIII

1. Introduction

    1.1 Research Background----------1

    1.2 Statement of the problem----------3

    1.3 Literature Review----------4

    1.4 Objective----------6

    1.5 Methodology----------7

    1.6 Thesis Outline----------8

2. Induction Motor Drive

    2.1 Dynamic Model of Induction motor ----------9

    2.2 Field Oriented Control----------10

    2.3 Energy Storage System----------12

    2.4 Speed and Flux Estimation of three phase induction motor----------14

2.5 Transformation Mechanisms----------25

2.6 PI controller----------31

2.7 Space Vector Pulse Width Modulation----------33

3. Regenerative braking analysis of induction machine

3.1 Different Breaking Methods----------39

3.2 Energy Balance during Regenerative Braking----------40

4. Simulation and Experimental Analysis

4.1 Overall System Analysis----------43

4.2 Results and Discussion ----------50

5. Conclusion and Future Work Recommendation

5.1 Conclusion ----------62

5.2 Future Recommendation----------62

Reference----------63

Appendix----------66

List of Tables

Table1: Device on/off patterns & resulting instantaneous voltage of a 3-ph power inverter------35

Table2: Switching patterns, corresponding space vectors &their dq-components----------36

Table3: SVPWM sector----------38

Table 4: Induction Motor and Control Parameters for Simulation and Experimentation----------47

Table5: Time data in braking IM----------61

List of Figures

Figure1- The waveforms of rotor flux angle in both directions----------18

Figure2-Clarke Transform----------26

Figure 3: Inverse Park Transform----------26

Figure4- Park Transform----------27

Figure5- Voltage Source Inverter with 3-ph electric motor----------28

Figure6-The abc-axis and stationary dq-axis components of the stator phase voltages----------31

Figure7-PI controller----------32

Figure8-Power circuit topology for a three-phase VSI----------34

Figure9-Basic space vectors----------36

Figure10- Power Analysis during Regenerative Braking----------42

Figure11-Overall System Block Diagram----------44

Figure12-Overall system of flux estimator----------45

Figure13-Simulink Model of Overall System----------47

Figure 14 Flux and Speed Estimation----------48

Figure 15 Voltage and Current Model Based Flux Estimation----------49

Figure 16 Bidirectional dc/dc Converter----------49

Figure 17 Direct Field Oriented Control----------50

Figure18-Variation of motor actual speed with regenerative braking----------50

Figure19-Variation of motor estimated speed with regenerative braking----------51

Figure20- Estimated rotor angle(theta)----------51

Figure21-Variation of motor torque with regenerative braking ----------52

Figure22-Variation of battery voltage with regenerative braking ----------52

Figure23-Variation of battery current with regenerative braking ----------53

Figure 24-Variation of battery power with regenerative braking ----------53

Figure 25-Variation of SOC of battery with regenerative braking ----------54

Figure 26- Energy Balance during regenerative braking ----------54

Figure 27- (a) Overall regenerative braking performance using battery with bidirectional dc/dc converter (b) Overall regenerative braking performance using battery without bidirectional dc/dc converter ----------55

Figure 28-Speed of IM at 0.3 pu----------57

Figure 29-Speed of IM decelerating to 0.2 pu ----------58

Figure 30-Speed of IM decelerating to 0.1 pu----------58

Figure 31-Speed of IM decelerating tozero----------59

Figure 32- Speed of IM at 0.4 pu----------60

Figure 33-Speed of IM decelerates to 0 pu----------60

Figure 34-Freefall and Regenerative braking time analysis----------61

List of Abbreviations

AC-Alternating current

DC-Direct current

FOC- Field Oriented Control

PWM- Pulse Width Modulation

VSI-Voltage Source Inverter

SPWM-Sinusoidal Pulse Width Modulation

SVPWM-Space Vector Pulse Width Modulation

IM-Induction Motor

HEVs-Hybrid Electric Vehicles

EVs-Electric Vehicles

NIMH-Nickel Metal Hydride

SOC-State of Charge

PI-Proportional Integral

PID-Proportional Integral Derivative

SVGEN- Space Vector Generator

DPWMmin- Dis-continous Pulse Width Modulation Minimization

PFC-Power Factor Correction

ACI- AC induction

PMSM- Permanent Magnet Synchronous Motor

BLDC-Brushless DC motor

ADC- Analog to Digital Converter

DAC-Digital to Analog Converter

IPM- Interior Permanent Magnet

CCW-Counter Clock Wise

CW-Clock Wise

p- Derivative operator

R_s- Stator resistance

L_m -magnetizing inductance

L_r -rotor inductance

L_s -stator inductance

T_r -rotor time constant

w_e –synchronous speed

w_r -rotor speed

V_{dse} -d-axis stator voltage

V_{qse} -q-axis stator voltage

i_{dse} - d-axis stator current in stationary reference frame

i_{qse} -q-axis stator current in stationary reference frame

λ_r – rotor flux

$V_{ddecoupling}$ –d-axis decoupling voltage

$V_{qdecoupling}$ -q-axis decoupling voltage

T_e -electromagnetic torque

P-number of poles

T_l –load torque

J-moment of Inertia

B-Coefficient of friction

V/HZ-Volts/Hrtz

E_o -Battery Constant Voltage

R-Internal Resistance

K-Polarization Constant

A-Exponential Zone Amplitude

B-Exponential Zone Time Constant Inverse

V_{batt}-Battery Voltage

Q-Battery Capacity

$\lambda_{dr}{}^{s}$ -d-axis rotor flux in stationary reference frame

$\lambda_{qr}{}^{s}$ -q-axis rotor flux in stationary reference frame

$i_{dr}{}^{s}$ -d-axis rotor current in stationary reference frame

$i_{qr}{}^{s}$ -q-axis rotor current in stationary reference frame

$i_{ds}{}^{s}$ -d-axis stator current in stationary reference frame

$i_{qs}{}^{s}$ –q-axis stator current in stationary reference frame

$\frac{d}{dt}$ - Derivative

$\lambda_{r}{}^{s}$ –rotor flux in stationary reference frame

$\theta_{\lambda r}$ -rotor flux angle

w_b -base speed

pu- per unit

f_b -base electrical frequency

T-sampling time

λ_b -base flux linkage

I_b -base current

$w_e{}^{\wedge}$ -filtered synchronous speed

τ_c -low pass filter time constant

f_c –cut-off frequency

$\psi_{dr}{}^{e,i}$ -d-axis rotor flux in synchronous rotating reference frame (current model)

$\psi_{qr}{}^{e,i}$-q-axis rotor flux synchronous rotating reference frame (current model)

$i_{ds}{}^{e}$ -d-axis stator current in synchronous rotating reference frame

$i_{qs}{}^{e}$ -q-axis stator current in synchronous rotating reference frame

$\psi_{r}{}^{e,i}$ -rotor flux in synchronously rotating reference frame

$\psi_{dr}{}^{s,i}$ -d-axis rotor flux in stationary reference frame (current model)

$\psi_{qr}^{s,i}$ -q-axis rotor flux in stationary reference frame (current model)

$\psi_{ds}^{s,i}$ -d-axis stator flux in stationary reference frame (current model)

$\psi_{qs}^{s,i}$ -q-axis stator flux in stationary reference frame (current model)

$\psi_{ds}^{s,v}$ -d-axis stator flux in stationary reference frame (voltage model)

$\psi_{qs}^{s,v}$ -q-axis stator flux in stationary reference frame (voltage model)

u_{ds} -d-axis stator voltage in stationary reference frame

u_{qs} -q-axis stator voltage in stationary reference frame

$u_{comp,ds}$ -d-axis stator compensated voltage

$u_{comp,qs}$ -q-axis stator compensated voltage

K_p –proportional gain

T_i -reset time

K_i -integral gain

$\psi_{dr}^{s,v}$ -d-axis rotor flux in stationary reference frame (voltage model)

$\psi_{qr}^{s,v}$ -q-axis rotor flux in stationary reference frame (voltage model)

e_{ds}^{s} -d-axis stationary back emf

e_{qs}^{s} -q-axis stationary back emf

V_{ds}^{s} - d-axis stator voltage in stationary reference frame

V_{qs}^{s} -q-axis stator voltage in stationary reference frame

V_{dc} -dc bus voltage

Chapter One
Introduction

1.1 Research Background

Regenerative braking refers to a process in which a portion of kinetic energy of the vehicle is stored by short term storage system or fed back to electrical system. Conventional braking systems convert kinetic energy into heat, usually via friction. This wastes a great amount of energy. Regenerative braking systems reclaim in storing the kinetic energy in a reusable manner. The main advantages of regenerative braking systems can be summarized as improved fuel economy, improved performance and Energy saving [1].

Vector control is becoming the industrial standard for induction motor control. The vector control technique decouples the two components of stator current space vector: one providing the control of flux and the other providing the control of torque. The two components are defined in the synchronously rotating reference frame. With the help of this control technique the induction motor can replace a separately excited dc motor. The vector control technique is therefore a better solution so that the control on flux and torque become independent from each other and the induction motor is transformed from a non-linear to linear control plant. With the advent of field oriented control; the induction motor has become an attractive option. Vector control is the main reason for regenerative braking to work below synchronous speed. Vector control can be classified as direct vector control and indirect vector control [2][3][4][5].

For control of IM a number of Pulse Width Modulation (PWM) schemes are used for vector control method. The most commonly used PWM schemes for three-phase voltage source inverters (VSI) are sinusoidal PWM (SPWM) and space vector PWM (SVPWM). Using space vector PWM (SVPWM) has advantage over other PWM schemes because it reduces harmonic content in voltage, Increase fundamental output voltage by 15% & smooth control of IM [6].
In this thesis a sensorless direct vector control method with Space Vector Pulse Width Modulation Technique (SVPWM) has been used.

Many modern electric drive vehicles including electric locomotives and HEVs have regenerative braking systems. The total amount of energy lost in this way depends on how often, how hard and how long the brakes are applied. One of the major area of research aims to develop strategies in order to increase the regeneration of power being wasted during braking. It increases efficiency of electric vehicle by saving of waste energy. In regenerative braking mode of electric vehicle the kinetic energy of wheels is converted into electricity and stored in batteries or capacitors.

This method is improved by using flywheel, DC-DC converter, ultra-capacitor as well as super capacitor [1][7][8].

In this thesis NIMH battery is connected to a bidirectional DC-DC converter in simulation. As in the case of motoring, the motor gets power from the battery and during regenerative braking the battery is charged by the power from the motor which used as generator to convert the kinetic energy of the motor to electrical energy and using power electronic device the ac power become converted to dc and store in the battery. Regenerative braking system and energy balance during regeneration are also analyzed.

1.2 Statement of the Problem

Although mechanical braking is a reliable braking method being used since the advent of vehicles, it dissipates the kinetic energy of the wheels. Electrical braking is an effective method which can be implemented along with the hydraulic braking for stop and go drive strategy in busy traffic. Plug braking and regenerative braking are two important methods of braking employed by the use of electric traction motor in EVs/HEVs. The method of plugging is efficient enough in terms of its fastness, but there was no regeneration of the kinetic energy into the battery during the process of braking. Due to the cost increasing in fuel products energy saving mechanism was necessary. Greenhouse effect was also another reason for efficient energy mechanism to be deployed. There in the concept of regenerative braking was evoked. During the process of regenerative braking, power is adaptively restored into the battery which improves the overall energy efficiency.

1.3 Literature Review

When a conventional vehicle applies its brakes, kinetic energy is converted to heat as friction between the brake pads and wheels. This energy is carries away in the airstream and energy is effectively wasted. Regenerative braking refers to a process in which a portion of kinetic energy of the vehicle is stored by short term storage system or fed back to the power supply. Energy normally dissipated in the brakes is directed by a power transmission system to the energy stored during deceleration.

The main advantages of regenerative braking systems can be summarized

- Improved fuel economy
- Improved performance
- Energy saving

The possible disadvantages of regenerative braking systems can be

- Complex control system
- Cost
- Noise: dependent on the system [1].

With Regenerative Braking Systems (RBS) it is possible to slow a vehicle down by converting its kinetic energy into electric energy, which can be either used immediately or stored until needed. This contrasts with conventional braking systems, where the excess kinetic energy is converted into heat by friction and wasted into the environment. In regenerative braking system of a HEV, the power electronics are controlled such that the traction motor operates as a generator to provide negative torque on the wheels and to produce electric energy [9][10].

The basic theory of solid-state slip-power-recovery systems is now well established. One of the disadvantages of such systems has been the lack of a suitable method of regenerative braking: this is frequently an important requirement for many applications. There are two methods of

incorporating regenerative braking in slip-power recovery systems. One method requires a separate source of direct current and is called the 'separately excited' regenerative brake; the second method employs direct current from the d.c. link in the system and is called the self-excited system [11].

As discussed above in regenerative braking mode of electric vehicle the kinetic energy of wheels and vehicle mass is converted into electricity and stored in batteries or capacitors. This method is improved by using flywheel, DC-DC converter, ultra-capacitor as well as super capacitor which significantly improve the rate of energy regeneration [7][8][12][13].

To achieve maximum energy recuperation it is advised to combine a regenerative braking with a conventional frictional braking system in an optimal way. Studies shows that in a vehicle with active regenerative braking control, a significant amount of braking energy can be recovered, and the brake system does not need much changing from the brake systems of conventional passenger cars [14].

1.4 Objective

General Objective: the aim of this research is to model, simulate and analyze regenerative braking of an induction motor.

Specific Objective: The research objective focuses:

- To model energy storage mechanism
- To analyze different aspects during regenerative braking
- To develop mathematical model of energy balance during regeneration
- To demonstrate basic concepts of regenerative braking using C2000 kit

1.5 Methodology

A vector control method is more efficient method in controlling the torque of an induction motor. Here direct field oriented control is used to control the torque and flux of induction motor. The speed and flux of IM are estimated using open loop speed estimator and voltage and current model based flux estimator. SVPWM technique is used for the PWM scheme in order to reduce the harmonics content in voltage.

A simulink model using Matlab simulink was developed for the system. The simulink model uses a battery model as a source and connect it to voltage source inverter through a bidirectional DC to DC converter then to IM. The simulink analysis of the overall system without a bidirectional dc/dc converter was compared to that of with a bidirectional dc/dc converter.

Using C2000 kit and reusable c code demonstration of braking has been analyzed. The different output waveforms for rotor angular velocity, the different values of torque producing current component i_{qs} and capacitor bank voltage were measured and analyzed to provide the demonstration of regenerative braking, and to gain some understanding of the dynamics within the regenerative braking process. In the experimental system the kit do not have a bidirectional dc to dc converter to see the generated back emf voltage during regenerative braking that is the increase in dc bus voltage. Therefore in this thesis an effort is made to demonstrate some basic concepts of regenerative braking by analyzing the torque producing current component and the dc bus voltage with decelerating speed and the comparison of time taken to brake a motor in regenerative mode and free fall.

1.6 Thesis Outline

This thesis contains five chapters.

Chapter I give an introductory preference to the thesis. The research background of the thesis is presented which motivated the researcher towards research objectives in field of regenerative braking of induction machine.

Chapter II provides Dynamic induction motor theory, energy storage mechanism, bidirectional dc-dc converter and equations used to mathematically describe the motor's behavior within this experiment. It also describes the mathematical expressions of each blocks used in the simulation and experiment.

Chapter III covers the regenerative braking analysis of IM. This includes different braking techniques, power system analysis during braking are discussed here.

Chapters IV contain overall system analysis, simulation and experimental results. It also contains limitations during experimentation.

Chapter V concludes the thesis with the information gained from the research, and provides recommendations for future follow on research in the development regenerative braking system.

Chapter Two
Induction Motor Drive

2.1Dynamic Model of Induction Motor

The control of an induction motor can be made similar to that of a DC machine with vector control technique, where it is possible to have independent control of flux and torque. In order to achieve it the mathematical model of the motor in a rotating reference frame has to be synchronized either to the stator, air gap or rotor flux vector. For this one should know the angle of the stator, air gap or rotor flux vector along with their magnitude [15].

The dynamic model of induction motor for rotor flux oriented vector control application can be written as follows

$$p\begin{bmatrix} id_{se} \\ iq_{se} \\ \lambda d_{re} \\ \lambda q_{re} \end{bmatrix} = \begin{bmatrix} \frac{-Rs}{\sigma Ls} & w_e & \frac{-Lm}{Lr\sigma Ls}p & \frac{w_e Lm}{Lr\sigma Ls} \\ -w_e & \frac{-Rs}{\sigma Ls} & \frac{-w_e Lm}{Lr\sigma Ls} & \frac{-Lm}{Lr\sigma Ls}p \\ \frac{Lm}{Tr} & 0 & \frac{-1}{Tr} & w_{sl} \\ 0 & \frac{Lm}{Tr} & -w_{sl} & \frac{-1}{Tr} \end{bmatrix} \begin{bmatrix} id_{se} \\ iq_{se} \\ \lambda d_{re} \\ \lambda q_{re} \end{bmatrix} + \begin{bmatrix} \frac{vd_{se}}{\sigma Ls} \\ \frac{vq_{se}}{\sigma Ls} \\ 0 \\ 0 \end{bmatrix} \quad (1)$$

Where id_{se} and iq_{se} are the stator currents and λd_{re} and λq_{re} the rotor fluxes in $d_e - q_e$ frame. Similarly R_s, L_s, R_r and L_r are the stator phase winding résistance, stator self-inductance, rotor winding resistance and the rotor self-inductance. The rotor time constant is given as $T_r = L_r / R_r$ and leakage inductance is σL_s where $\sigma = 1 - (L_m^2 / L_s L_r)$.

For rotor flux oriented control the rotor flux λ_r is directed along the *d*-axis and is equal to λd_{re} and therefore $\lambda q_{re} = 0$. Thus equation (1a) modifies as shown below

$$\begin{bmatrix} id_{se} \\ iq_{se} \\ p\lambda d_{re} \\ 0 \end{bmatrix} = \begin{bmatrix} \frac{-Rs}{\sigma Ls} & w_e \frac{-Lm}{Lr\sigma Ls} p & 0 \\ -w_e & \frac{-Rs}{\sigma Ls} \frac{-w_e Lm}{Lr\sigma Ls} & 0 \\ \frac{Lm}{Tr} & 0 & \frac{-1}{Tr} \\ 0 & 0 & 0 \end{bmatrix} \begin{bmatrix} id_{se} \\ iq_{se} \\ \lambda d_{re} \\ 0 \end{bmatrix} + \begin{bmatrix} \frac{vd_{se}}{\sigma Ls} \\ \frac{vq_{se}}{\sigma Ls} \\ 0 \\ 0 \end{bmatrix} \quad (2)$$

From equation (1b) it can be seen that the $d_e - q_e$axis voltage are coupled by the terms

$$V_d decoupling = -\sigma L_s w_e iq_{se} \quad (3)$$

$$V_q decoupling = \sigma L_s w_e id_{se} + \frac{L_m}{L_r} w_e \lambda d_{re} \quad (4)$$

The electromagnetic torque equation of a rotor flux oriented is given as

$$T_e = \frac{3}{2}\frac{P}{2}\frac{L_m}{L_r} iq_{se}\lambda d_{re} \quad (5)$$

$$\text{Also} T_e = T_l + \frac{Jdw_r}{dt} + Bw_r \quad (6)$$

Where T_l, J, B and $w_r$are the load torque, moment of inertia, coefficient of friction and rotor speed respectively. From equation (2e) and (2f) the transfer function of the speed controller is given as

$$\frac{w_r}{T_e} = \frac{\frac{1}{J}}{s+\frac{B}{J}} \quad (7)$$

2.2 Field Oriented Control

A simple control such as the V/Hz strategy has limitations on the performance. To achieve better dynamic performance, a more complex control scheme needs to be applied, to control the induction motor. The advanced control strategy, which use mathematical transformations in order to decouple the torque generation and the magnetization functions in an AC induction motor is commonly called rotor flux oriented control, or simply Field Oriented Control (FOC).

The Field Orientated Control consists of controlling the stator currents represented by a vector. This control is based on projections which transform a three phase time and speed dependent system into a two co-ordinate (d and q co-ordinates) time invariant system. These projections lead to a structure similar to that of a DC machine control. Field orientated controlled machines need two constants as input references: the torque component (aligned with the q co-ordinate) and the flux component (aligned with d co-ordinate). As Field Orientated Control is simply based on projections the control structure handles instantaneous electrical quantities. This makes the control accurate in every working operation (steady state and transient) and independent of the limited bandwidth mathematical model.

By maintaining the amplitude of the rotor flux λ_r at a fixed value we have a linear relationship between torque and torque component (i_{sq}). We can then control the torque by controlling the torque component of stator current vector [16]. Field oriented control can be classified as Indirect field oriented control (IFOC) and Direct field oriented control (DFOC).

In indirect vector control technique, the rotor position is calculated from the speed feedback signal of the motor. This technique eliminates most of the problems, which are associated with the flux sensors as they are absent [3][17].

Direct vector control method determines the magnitude and position of the rotor flux vector by direct flux measurement or estimation. The flux is measured by the sensors like Hall Effect sensor, search coil and this is a part of the disadvantages. Because fixing of number of sensors is a tedious job and this increases the cost factor [3].The quantities generated from flux sensors are used in the outer loop of the drive control structure.
Alternatively, in place of flux sensors, the flux models can also be used for which the stator currents and voltages become the feedback signals and the rotor flux angle is given as its estimated output.

In this thesis sensorless direct field oriented control is used. The torque and the flux are controlled with PI controller. Since in direct field oriented control the estimation of the rotor position is necessary in this thesis both voltage and current model flux estimation technique is used. The speed is estimated using an open loop speed estimator.

2.3 Energy Storage Mechanism

The energy storage system stores energy generated during braking and discharges it when the motor accelerates. It also stabilizes the system voltage. There are different energy storage units such as super capacitors, batteries and flywheel.

Super capacitors are electrochemical capacitors that have an unusually high energy density when compared to common capacitors, typically on the order of thousands of times greater than a high capacity electrolytic capacitor. They can be used to applications normally reserved for batteries.

Battery Model

For the purpose of EVs and HEVs, batteries are the primary means of energy storage. In the use of HEVs, rechargeable batteries are used which deliver energy to the machine system(discharging) while cruising, accept energy from the system (charging) during regenerative braking and also store energy when not in use(storage). For the application in automobile industries, batteries should be efficient in terms of specific power, specific energy, efficiency, safety, cost, maintenance requirement and environmental adaptability [18].

The two primary modeling strategies for the battery are the circuit oriented modeling and the mathematical modeling. Circuit oriented battery models use a combination of voltage and current sources, resistors and capacitors to model the battery performance. The various basic forms include the

1. Thevenin Based Model
2. Impedance Based Model
3. Runtime Based Model

However, such models are complicated enough to determine battery parameters and the state of charge of the battery in account for variations between the charge and the discharge state which requires two opposing diodes. This makes the system even more complex. The mathematical modeling is based on Shepherd equation and Peukerts model. The voltage –current model describing the change of the terminal voltage with respect to current is the most vital sub model. This model usually starts from the basic Shepherd Equation and then the relation is improved to

fit to the charge and discharge curve. Here Mathematical model of the Nickel-Metal-Hydride battery which is most widely used for applications in EVs and HEVs has been used.

The battery voltage, the battery current, battery power and the state of charge (SOC) of the battery are chosen as state variables to depict the performance of the battery both during the charging and the discharging phenomenon.

The Shepherd model describes the electrochemical behavior of the battery in terms of the terminal voltage, open circuit voltage, internal resistance, discharge current and state of charge [18]. This model is well defined for both the charge and discharge characteristics. The mathematical model based on Shepherd model available in Matlab/SimPowerSystems for Nickel Metal Hydride model has been used.

Charge model

(i*<0): $E_0 - K * \frac{Q}{|it|+0.1*Q} * i * -k\frac{Q}{Q-it} * it + Laplace^{-1}\left[\frac{Exp(s)}{Sel(s)}\frac{1}{s}\right]$

Discharge model

(i*>0): $E_0 - K * \frac{Q}{Q-it} * i - k\frac{Q}{Q-it} * it + Laplace^{-1}\left[\frac{Exp(s)}{Sel(s)}.0\right]$

The following assumptions are made in the modeling of the battery

- During both charging and discharging the internal resistance remains constant and independent of the amplitude of the current
- The parameters are extracted from the discharge characteristics and are assumed to remain the same for charging.
- The battery capacity remains independent of the amplitude of the current (No Peukert effect).
- The temperature has no effect on the behavior of the model
- The self-discharge of the battery is not represented
- There is no memory effect on the model

The following are the limitations in the design of the battery model

- The minimum no load battery voltage is 0 V and the maximum voltage is 2*E_oV.
- The minimum capacity of the battery is 0 Ah and the maximum capacity is Q.
- The maximum SOC cannot be greater than 100% if the battery is over-charged.

A Nickel Metal-Hydride has been used as the energy source for this thesis work. Taking a battery with nominal voltage = 1.2V, rated capacity = 6.5 Ah and battery response time of 30s as given in[18] the discharge curve is used to extract the parameters E_o, R, K, A and B

Where E_o=1.2816VR=0.002K=0.0014A=0.111B=2.3077

2.4 Speed and Flux Estimation of Three Phase Induction Motor

Speed Estimation

Description: This block implements a speed estimator of the 3-ph induction motor based upon its mathematical model. The estimator's accuracy relies heavily on knowledge of critical motor parameters

The open-loop speed estimator is derived basing on the mathematical equations of induction motor in the stationary reference frame. The precise values of machine parameters are unavoidably required; otherwise the steady-state speed error may happen. However, the structure of the estimator is much simple comparing with other advanced techniques [19].All equations represented here are in the stationary reference frame (with superscript "s"). Firstly, the rotor flux linkage equations can be shown as below:

$$\lambda_{dr}{}^{s}=L_r i_{dr}{}^{s}+L_m i_{ds}{}^{s} \quad (1)$$

$$\lambda_{qr}{}^{s} = L_r i_{qr}{}^{s}+L_m i_{qs}{}^{s} \quad (2)$$

where L_r, and L_m are rotor, and magnetizing inductance (H), respectively.

According to Equations (1)-(2), the rotor currents can be expressed as

$$i_{dr}{}^{s} = \frac{1}{L_r}(\lambda_{dr}{}^{s} - L_m i_{ds}{}^{s}) \quad (3)$$

$$i_{qr}{}^{s} = \frac{1}{L_r}(\lambda_{qr}{}^{s} - L_m i_{qs}{}^{s}) \quad (4)$$

Secondly, the rotor voltage equations are used to find the rotor flux linkage dynamics

$$0 = R_r {i_{dr}}^s + \omega_r {\lambda_{qr}}^s + \frac{d{\lambda_{dr}}^s}{dt} \tag{5}$$

$$0 = R_r {i_{qr}}^s - \omega_r {\lambda_{dr}}^s + \frac{d{\lambda_{qr}}^s}{dt} \tag{6}$$

where ω_r is electrically angular velocity of rotor (rad/sec), and R_r is rotor resistance (Ω).

Substituting the rotor currents from Equations (3)-(4) into Equations (5)-(6), then the rotor flux linkage dynamics can be found as

$$\frac{d{\lambda_{dr}}^s}{dt} = -\frac{1}{\tau_r}{\lambda_{dr}}^s + \frac{L_m}{\tau_r}{i_{ds}}^s - \omega_r {\lambda_{qr}}^s \tag{7}$$

$$\frac{d{\lambda_{qr}}^s}{dt} = -\frac{1}{\tau_r}{\lambda_{qr}}^s + \frac{L_m}{\tau_r}{i_{qs}}^s - \omega_r {\lambda_{dr}}^s \tag{8}$$

Where $\tau_r = \frac{L_r}{R_r}$ is rotor time constant (sec).

Suppose that the rotor flux linkages in Equations (7)-(8) are known, therefore, its magnitude and angle can be computed as

$${\lambda_r}^s = \sqrt{({\lambda_{dr}}^s)^2 + ({\lambda_{qr}}^s)^2} \tag{9}$$

$$\theta_{\lambda_r} = tan^{-1}\left(\frac{{\lambda_{qr}}^s}{{\lambda_{dr}}^s}\right) \tag{10}$$

Next, the rotor flux (i.e., synchronous) speed;ω_e can be easily calculated by derivative of the rotor flux angle in Equation (10).

$$\omega_e = \frac{d\theta_{\lambda_r}}{dt} = \frac{dtan^{-1}\left(\frac{{\lambda_{qr}}^s}{{\lambda_{dr}}^s}\right)}{dt} \tag{11}$$

Referring to the derivative table, Equation (11) can be solved as

$$\frac{d(tan^{-1}u)}{dt} = \frac{1}{1+u^2}\frac{du}{dt} \tag{12}$$

Where u=$\frac{\lambda_{qr}{}^{s}}{\lambda_{dr}{}^{s}}$ yields,

$$\omega_e = \frac{d\theta_{\lambda_r}}{dt} = \frac{(\lambda_{dr}{}^{s})^2}{(\lambda_r{}^{s})^2}\left(\frac{\lambda_{dr}{}^{s}\left(\frac{d\lambda_{qr}{}^{s}}{dt}\right)-\lambda_{qr}{}^{s}\left(\frac{d\lambda_{dr}{}^{s}}{dt}\right)}{(\lambda_{dr}{}^{s})^2}\right) \tag{13}$$

Substituting Equations (7)-(8) into Equation (13), and rearranging, then finally it gives

$$\omega_e = \frac{d\theta_{\lambda_r}}{dt} = \omega_r + \frac{1}{(\lambda_r{}^{s})^2}\frac{L_m}{\tau_r}(\lambda_{dr}{}^{s} i_{qs}{}^{s} - \lambda_{qr}{}^{s} i_{ds}{}^{s}) \tag{14}$$

The second term of the right hand in Equation (14) is known as slip that is proportional to the electromagnetic torque when the rotor flux magnitude is maintaining constant. The electromagnetic torque can be shown here for convenience.

$$T_e = \frac{3}{2}\frac{p}{2}\frac{L_m}{L_r}(\lambda_{dr}{}^{s} i_{qs}{}^{s} - \lambda_{qr}{}^{s} i_{ds}{}^{s}) \tag{15}$$

where p is the number of poles. Thus, the rotor speed can be found as

$$\omega_r = \omega_e - \frac{1}{(\lambda_r{}^{s})^2}\frac{L_m}{\tau_r}(\lambda_{dr}{}^{s} i_{qs}{}^{s} - \lambda_{qr}{}^{s} i_{ds}{}^{s}) \tag{16}$$

Now, the per-unit concept is applied to Equation (16), then, Equation (16) becomes

$$\omega_{r,pu} = \omega_{e,pu} - \frac{1}{\omega_b \tau_r}\frac{(\lambda_{dr,pu}{}^{s} i_{qs,pu}{}^{s} - \lambda_{qr,pu}{}^{s} i_{ds,pu}{}^{s})}{(\lambda_{r,pu}{}^{s})^2}\text{pu} \tag{17}$$

Where$\omega_b = 2\Pi f_b$is the base electrically angular velocity (rad/sec), $\lambda_b = L_m I_b$is the base flux linkage (volt.sec), and I_b is the base current (amp). Equivalently, another form is

$$\omega_{r,pu} = \omega_{e,pu} - K_1\left(\frac{(\lambda_{dr,pu}{}^{s} i_{qs,pu}{}^{s} - \lambda_{qr,pu}{}^{s} i_{ds,pu}{}^{s})}{(\lambda_{r,pu}{}^{s})^2}\right)\text{pu} \tag{18}$$

Where $K_1 = \frac{1}{\omega_b \tau_r}$

The per-unit synchronous speed can be calculated as

$$\omega_{e,pu} = \frac{1}{2\Pi f_b}\frac{d\theta_{\lambda_r}}{dt} = \frac{1}{f_b}\frac{d\theta_{\lambda_{r,pu}}}{dt}\text{pu} \quad (19)$$

where f_b is the base electrical (supplied) frequency (Hz) and 2π is the base angle (rad). Discretizing Equation (19) by using the backward approximation, yields

$$\omega_{e,pu}(k) = \frac{1}{f_b}\{\frac{\theta_{\lambda_{r,pu}}(k)-\theta_{\lambda_{r,pu}}(k-1)}{T}\}\text{pu} \quad (20)$$

where T is the sampling period (sec). Equivalently, another form is

$$\omega_{e,pu}(k) = k_2(\theta_{\lambda_{r,pu}}(k) - \theta_{\lambda_{r,pu}}(k-1)\text{pu} \quad (21)$$

Where $k_2 = \frac{1}{f_b T}$ is usually a large number.

In practice, the typical waveforms of the rotor flux angle, $\theta_{\lambda_{r,pu}}$ in both directions can be seen in Figure 1. To take care the discontinuity of angle from 360^0 to 0^0 (CCW) or from 0^0 to 360^0 (CW), the differentiator is simply operated only within the differentiable range as seen in this Figure 1. This differentiable range does not significantly lose the information to compute the estimated speed.

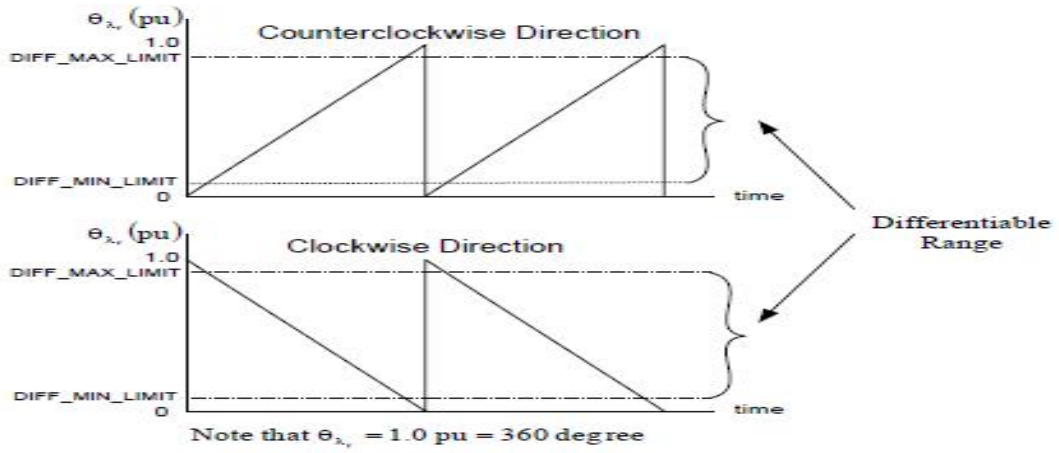

Figure1: The waveforms of rotor flux angle in both directions[19]

In addition, the synchronous speed in Equation (21) is necessary to be filtered out by a low-pass filter in order to reduce the amplifying noise generated by the pure differentiator in Equation (21). A simple 1st-order low-pass filter is used.The actual synchronous speed to be used is the

output of the low-pass filter$\hat{\omega}_{e,pu}$, seen in following equation. The continuous-time equation of 1st-order low-pass filter is as

$$\frac{d\hat{\omega}_{e,pu}}{dt} = \frac{1}{\tau_c}(\omega_{e,pu} - \hat{\omega}_{e,pu}) \tag{22}$$

Where$\tau_c = \frac{1}{2\Pi f_c}$is the low-pass filter time constant (sec), and f_c is the cut-off frequency (Hz). Using backward approximation, then Equation (22) finally becomes

$$\hat{\omega}_{e,pu}(k) = k_3\hat{\omega}_{e,pu}(k-1) + k_4\omega_{e,pu}(k)\text{pu} \tag{23}$$

Where $k_3 = \frac{\tau_c}{\tau_c+T}andk_4 = \frac{T}{\tau_c+T}$. In fact, only three Equations (18), (21), and (23) are mainly employed to compute the estimated speed in per-unit.

Flux Estimation

Description: This block implements the flux estimator with the rotor flux angle for the 3-ph induction motor based upon the integral of back emf's (voltage model) approach.

Continuous Time:

Firstly, the rotor flux linkage dynamics in synchronously rotating reference frame ($\omega = \omega_e = \omega_{\psi_r}$) can be shown as below:

$$\frac{d\psi_{dr}^{e,i}}{dt} = \frac{L_m}{\tau_r} i_{ds}^{e} - \frac{1}{\tau_r}\psi_{dr}^{e,i} + (\omega_e - \omega_r)\psi_{qr}^{e,i} \tag{1}$$

$$\frac{d\psi_{qr}^{e,i}}{dt} = \frac{L_m}{\tau_r} i_{qs}^{e} - \frac{1}{\tau_r}\psi_{qr}^{e,i} + (\omega_e - \omega_r)\psi_{dr}^{e,i} \tag{2}$$

where L_m is the magnetizing inductance (H), $\tau_r = \frac{L_r}{R_r}$ is the rotor time constant (sec), and w_r is the electrically angular velocity of rotor (rad/sec)[19].

In the current model, total rotor flux linkage is aligned into the d-axis component, which is modeled by the stator currents, thus

$$\psi_r{}^{e,i} = \psi_{dr}{}^{e,i} \text{ and } \psi_{qr}{}^{e,i} = 0 \quad (3)$$

Substituting $\psi_{qr}{}^{e,i} = 0$ into Equations (1)-(2), yields the oriented rotor flux dynamics are

$$\frac{d\psi_{dr}{}^{e,i}}{dt} = \frac{L_m}{\tau_r} i_{ds}{}^{e} - \frac{1}{\tau_r}\psi_{dr}{}^{e,i} \quad (4)$$

$$\psi_{qr}{}^{e,i} = 0 \quad (5)$$

Note that Equation (4) and (5) are the classical rotor flux vector control equations. Then, the rotor flux linkages in Equation (4)-(5) are transformed into the stationary reference frame performed by inverse park transformation.

$$\psi_{dr}{}^{s,i} = \psi_{dr}{}^{e,i} \cos\theta_{\psi_r} - \psi_{qr}{}^{e,i} \sin\theta_{\psi_r} = \psi_{dr}{}^{e,i} \cos\theta_{\psi_r} \quad (6)$$

$$\psi_{qr}{}^{s,i} = \psi_{dr}{}^{e,i} \sin\theta_{\psi_r} + \psi_{qr}{}^{e,i} \cos\theta_{\psi_r} = \psi_{dr}{}^{e,i} \sin\theta_{\psi_r} \quad (7)$$

Where θ_{ψ_r} is the rotor flux angle (rad).

Then, the stator flux linkages in stationary reference frame are computed from the rotor flux linkages in Equation (6)-(7)

$$\psi_{ds}{}^{s,i} = L_s i_{ds}{}^{s} + L_m i_{dr}{}^{s} = \left(\frac{L_s L_r - L_m{}^2}{L_r}\right) i_{ds}{}^{s} + \frac{L_m}{L_r}\psi_{dr}{}^{s,i} \quad (8)$$

$$\psi_{qs}{}^{s,i} = L_s i_{qs}{}^{s} + L_m i_{qr}{}^{s} = \left(\frac{L_s L_r - L_m{}^2}{L_r}\right) i_{qs}{}^{s} + \frac{L_m}{L_r}\psi_{qr}{}^{s,i} \quad (9)$$

Where L_s and L_r are the stator and rotor self inductance (H), respectively.

Next, the stator flux linkage in the voltage model is computed by means of back emf's integration with compensated voltages.

$$\psi_{ds}{}^{s,v} = \int (u_{ds}{}^{s} - i_{ds}{}^{s} R_s - u_{comp,ds}) dt \quad (10)$$

$$\psi_{qs}{}^{s,v} = \int (u_{qs}{}^{s} - i_{qs}{}^{s} R_s - u_{comp,qs}) dt \quad (11)$$

where R_s is the stator resistance (Ω), ${u_{ds}}^s, {u_{qs}}^s$ are stationary dq-axis stator voltages, and the compensated voltages are computed by the PI control law as follows:

$$u_{comp,ds} = K_p({\psi_{ds}}^{s,v} - {\psi_{ds}}^{s,i}) + \frac{K_p}{T_I}\int({\psi_{ds}}^{s,v} - {\psi_{ds}}^{s,i})\mathrm{dt} \quad (12)$$

$$u_{comp,qs} = K_p({\psi_{qs}}^{s,v} - {\psi_{qs}}^{s,i}) + \frac{K_p}{T_I}\int({\psi_{qs}}^{s,v} - {\psi_{qs}}^{s,i})\mathrm{dt} \quad (13)$$

The proportional gain K_p and the reset time T_I are chosen such that the flux linkages computed by current model is domínant at low speed because the back emf's computed by the voltage model are extremely low at this speed range (even zero back emf's at zero speed). While at high speed range, the flux linkages computed by voltage model is dominant[19].

Once the stator flux linkages in Equation (10)-(11) are calculated, the rotor flux linkages based on the voltage model are further computed, by rearranging Equation (8)-(9), as

$${\psi_{dr}}^{s,v} = -(\frac{L_s L_r - {L_m}^2}{L_m}){i_{ds}}^s + \frac{L_r}{L_m}{\psi_{ds}}^{s,v} \quad (14)$$

$${\psi_{qr}}^{s,v} = -(\frac{L_s L_r - {L_m}^2}{L_n}){i_{qs}}^s + \frac{L_r}{L_n}{\psi_{qs}}^{s,v} \quad (15)$$

Then, the rotor flux angle based on the voltage model is finally computed as

$$\theta_{\psi_r} = tan^{-1}(\frac{{\psi_{qr}}^{s,v}}{{\psi_{dr}}^{s,v}}) \quad (16)$$

Discrete Time:

The oriented rotor flux dynamics in Equation (4) is discretized by using backward approximation as follows:

$$\frac{{\psi_{dr}}^{e,i}(k) - {\psi_{dr}}^{e,i}(k-1)}{T} = \frac{L_m}{\tau_r}{i_{ds}}^e(k) - \frac{1}{\tau_r}{\psi_{dr}}^{e,i}(k) \quad (17)$$

where T is the sampling period (sec). Rearranging (17), then it gives

$${\psi_{dr}}^{e,i}(k) = (\frac{\tau_r}{\tau_r + T}){\psi_{dr}}^{e,i}(k-1) + (\frac{L_m T}{\tau_r + T}){i_{ds}}^e(k) \quad (18)$$

Next, the stator flux linkages in Equation (10)-(11) are discretized by using trapezoidal (or tustin) approximation as

$$\psi_{ds}{}^{s,v}(k) = \psi_{ds}{}^{s,v}(k-1) + \frac{T}{2}(e_{ds}{}^{s}(k) + e_{ds}{}^{s}(k-1)) \tag{19}$$

$$\psi_{qs}{}^{s,v}(k) = \psi_{qs}{}^{s,v}(k-1) + \frac{T}{2}(e_{qs}{}^{s}(k) + e_{qs}{}^{s}(k-1)) \tag{20}$$

where the back emf's are computed as

$$e_{ds}{}^{s}(k) = u_{ds}{}^{s}(k) - i_{ds}{}^{s}(k)R_s - u_{comp,ds}(k) \tag{21}$$

$$e_{qs}{}^{s}(k) = u_{qs}{}^{s}(k) - i_{qs}{}^{s}(k)R_s - u_{comp,qs}(k) \tag{22}$$

Similarly, the PI control laws in Equation (12)-(13) are also discretized by using trapezoidal approximation as

$$u_{comp,ds}(k) = K_p(\psi_{ds}{}^{s,v}(k) - \psi_{ds}{}^{s,i}(k)) + u_{comp,ds,i}(k-1) \tag{23}$$

$$u_{comp,qs}(k) = K_p(\psi_{qs}{}^{s,v}(k) - \psi_{qs}{}^{s,i}(k)) + u_{comp,qs,i}(k-1) \tag{24}$$

where the accumulating integral terms are as

$$u_{comp,ds,i}(k) = u_{comp,ds,i}(k-1) + \frac{K_pT}{T_I}(\psi_{ds}{}^{s,v}(k) - \psi_{ds}{}^{s,i}(k))$$

$$= u_{comp,ds,i}(k-1) + K_PK_I(\psi_{ds}{}^{s,v}(k) - \psi_{ds}{}^{s,i}(k)) \tag{25}$$

$$u_{comp,qs,i}(k) = u_{comp,qs,i}(k-1) + \frac{K_pT}{T_I}(\psi_{qs}{}^{s,v}(k) - \psi_{qs}{}^{s,i}(k))$$

$$= u_{comp,qs,i}(k-1) + K_PK_I(\psi_{qs}{}^{s,v}(k) - \psi_{qs}{}^{s,i}(k)) \tag{26}$$

Where $K_I = \frac{T}{T_I}$

Discrete Time and Per Unit

Now all equations are normalized into the per-unit by the specified base quantities. Firstly, the rotor flux linkage in current model in Equation (18) is normalized by dividing the base flux linkage as

$$\psi_{dr,pu}{}^{e,i}(K) = (\frac{\tau_r}{\tau_r+T})\psi_{dr,pu}{}^{e,i}(k-1) + \left(\frac{T}{\tau_r+T}\right) i_{ds,pu}{}^{e}(k)\text{pu} \quad (27)$$

Where $\psi_b = L_m I_b$ is the base flux linkage (volt.sec) and I_b is the base current (amp).

Next, the stator flux linkages in the current model in Equation (8)-(9) are similarly normalized by dividing the base flux linkage as

$$\psi_{ds,pu}{}^{s,i}(k) = \left(\frac{L_s L_r - L_m{}^2}{L_r L_m}\right) i_{ds,pu}{}^{s}(k) + \frac{L_m}{L_r}\psi_{dr,pu}{}^{s,i}(k) \quad \text{pu} \quad (28)$$

$$\psi_{qs,pu}{}^{s,i}(k) = \left(\frac{L_s L_r - L_m{}^2}{L_r L_n}\right) i_{qs,pu}{}^{s}(k) + \frac{L_m}{L_r}\psi_{qr,pu}{}^{s,i}(k) \quad \text{pu} \quad (29)$$

Then, the back emf's in Equation (21)-(22) are normalized by dividing the base phase voltage V_b

$$e_{ds,pu}{}^{s}(k) = u_{ds,pu}{}^{s}(k) - \frac{I_b R_s}{V_b} * i_{ds,pu}{}^{s}(k)R_s - u_{comp,ds,pu}(k) \quad (30)$$

$$e_{qs,pu}{}^{s}(k) = u_{qs,pu}{}^{s}(k) - \frac{I_b R_s}{V_b} * i_{qs,pu}{}^{s}(k)R_s - u_{comp,qs,pu}(k) \quad (31)$$

Next, the stator flux linkages in the voltage model in Equation (19)-(20) are divided by the base flux linkage.

$$\psi_{ds,pu}{}^{s,v}(k) = \psi_{ds,pu}{}^{s,v}(k-1) + \frac{V_b T}{L_m I_b}\left(\frac{e_{ds,pu}{}^{s}(k) + e_{ds,pu}{}^{s}(k-1)}{2}\right) \quad (32)$$

$$\psi_{qs,pu}{}^{s,v}(k) = \psi_{qs,pu}{}^{s,v}(k-1) + \frac{V_b T}{L_n I_b}\left(\frac{e_{qs,pu}{}^{s}(k) + e_{qs,pu}{}^{s}(k-1)}{2}\right) \quad (33)$$

Similar to Equation (28)-(29), the normalized rotor flux linkages in voltage model are

$$\psi_{dr,pu}{}^{s,v}(k) = -\left(\frac{L_s L_r - L_m{}^2}{L_n L_n}\right) i_{ds,pu}{}^{s}(k) + \frac{L_r}{L_n}\psi_{ds,pu}{}^{s,v}(k) \quad (34)$$

$$\psi_{qr,pu}{}^{s,v}(k) = -(\frac{L_s L_r - L_m{}^2}{L_n L_n})i_{qs,pu}{}^{s}(k) + \frac{L_r}{L_n}\psi_{qs,pu}{}^{s,v}(k) \quad (35)$$

Inconclusion, the discrete-time, per-unit equations are rewritten in terms of constants.

Current model – rotor flux linkage in synchronously rotating reference frame ($\omega=\omega_{\psi_r}$)

$$\psi_{dr,pu}{}^{e,i}(k) = K_1\psi_{dr,pu}{}^{e,i}(k-1) + K_2 i_{ds,pu}{}^{e}(k)pu \quad (36)$$

Where $K_1 = \frac{\tau_r}{\tau_r+T}$ and$K_2 = \frac{T}{\tau_r+T}$

Current model – rotor flux linkages in the stationary reference frame ($\omega=0$)

$$\psi_{ds,pu}{}^{s,i}(k) = K_4 i_{ds,pu}{}^{s}(k) + K_3\psi_{dr,pu}{}^{s,i}(k)pu \quad (37)$$

$$\psi_{qs,pu}{}^{s,i}(k) = K_4 i_{qs,pu}{}^{s}(k) + K_3\psi_{qr,pu}{}^{s,i}(k)pu \quad (38)$$

Where $K_3 = \frac{L_m}{L_r}$ and $K_4 = \frac{L_s L_r - L_m{}^2}{L_r L_m}$

Voltage model – back emf's in the stationary reference frame ($\omega=0$)

$$e_{ds,pu}{}^{s}(k) = u_{ds,pu}{}^{s}(k) - K_5 i_{ds,pu}{}^{s}(k) - u_{comp,ds,pu}(k)\text{pu} \quad (39)$$

$$e_{qs,pu}{}^{s}(k) = u_{qs,pu}{}^{s}(k) - K_5 i_{qs,pu}{}^{s}(k) - u_{comp,qs,pu}(k)\text{pu} \quad (40)$$

Where$K_5 = \frac{I_b R_s}{V_b}$

Voltage model - stator flux linkages in the stationary reference frame ($\omega=0$)

$$\psi_{ds,pu}{}^{s,v}(k) = \psi_{ds,pu}{}^{s,v}(k-1) + \mathrm{K}_6(\frac{e_{ds,pu}{}^{s}(k)+e_{ds,pu}{}^{s}(k-1)}{2})\ \text{pu} \quad (41)$$

$$\psi_{qs,pu}{}^{s,v}(k) = \psi_{qs,pu}{}^{s,v}(k-1) + \mathrm{K}_6(\frac{e_{qs,pu}{}^{s}(k)+e_{qs,pu}{}^{s}(k-1)}{2})\ \text{pu} \quad (42)$$

Where $K_6 = \frac{V_b T}{L_n I_b}$

Voltage model – rotor flux linkages in the stationary reference frame (ω=0)

$$\psi_{dr,pu}{}^{s,v}(k) = -K_8 i_{ds,pu}{}^{s} + K_7 \psi_{ds,pu}{}^{s,v}(k)\text{pu} \quad (43)$$

$$\psi_{qr,pu}{}^{s,v}(k) = -K_8 i_{qs,pu}{}^{s} + K_7 \psi_{qs,pu}{}^{s,v}(k)\text{pu} \quad (44)$$

Where $K_7 = \frac{L_r}{L_m}$ and $K_8 = \frac{L_s L_r - L_m{}^2}{L_m L_m}$

Voltage model – rotor flux angle

$$\theta_{\psi_{r,pu}}(k) = \frac{1}{2\Pi}\tan^{-1}\left(\frac{\psi_{qr,pu}{}^{s,v}(k)}{\psi_{dr,pu}{}^{s,v}(k)}\right) \text{ pu} \quad (45)$$

Notice that the rotor flux angle is computed by a look-up table of 0-45 degree with 256 entries.

In fact, Equations (36)-(44) are mainly employed to compute the estimated flux linkages in per-unit.

2.5Transformation Mechanisms

Clarke Transform

*Description:*Converts balanced three phase quantities into balanced two phase quadrature quantities[19].

Here it is assumed that all three phases are balanced (i.e. $i_a + i_b + i_c = 0$) and they have positive sequence (ABC) as follows:

$$I_a = I * \cos(\omega t) \quad (1)$$

$$I_b = I * \cos(\omega t - 2\Pi/3) \quad (2)$$

$$I_c = I * \cos(\omega t - 4\Pi/3) \quad (3)$$

This macro implements the following equations:

$$I_\alpha = I_a \tag{4}$$

$$I_\beta = (2I_b + I_a)/\sqrt{3} \tag{5}$$

Which result in

$$I_\alpha = I * \cos(\omega t) \tag{6}$$

$$I_\beta = I * \sin(\omega t) \tag{7}$$

This transformation converts balanced three phase quantities into balanced two phase quadrature quantities as shown in figure below.

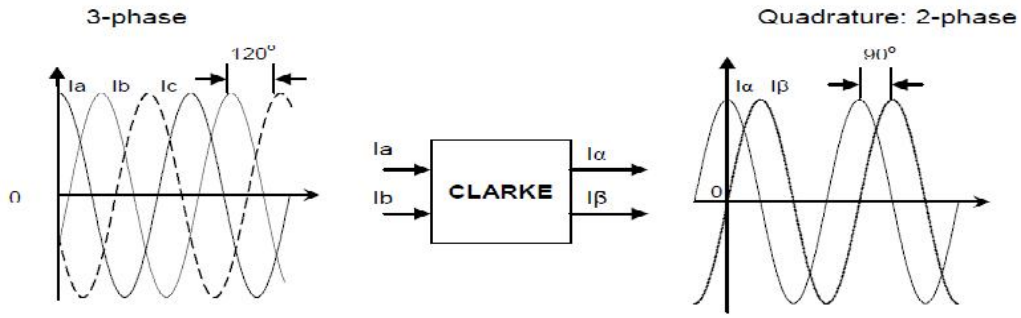

Figure 2 Clarke transforms[19]

Inverse Park Transform

Description: This transformation projects vectors in orthogonal rotating reference frame into two phase orthogonal stationary frame[19].

It Implements the following equations:

$$I_a = I_D * cos\theta - I_Q * sin\theta \tag{1}$$

$$I_q = I_D * sin\theta + I_Q * cos\theta \tag{2}$$

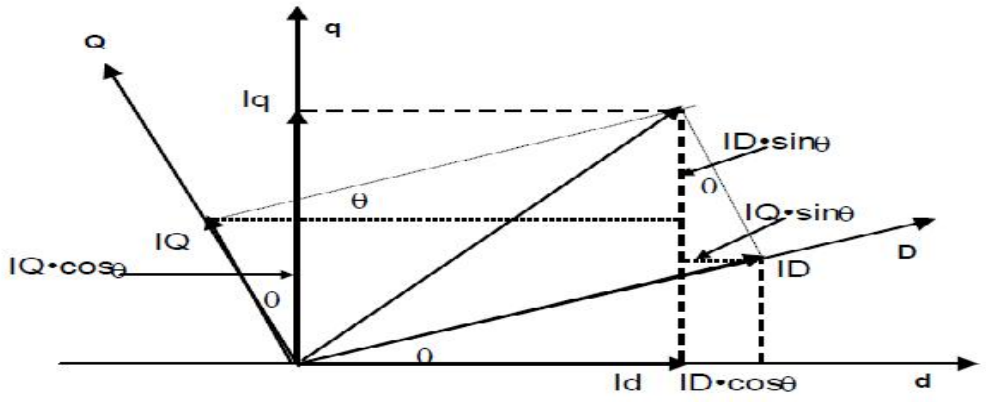

Figure 3. Inverse park transform[19]

Park Transform

*Description:*This transformation converts vectors in balanced 2-phase orthogonal stationary system into orthogonal rotating reference frame[19].

It Implements the following equations:

$$I_D = I_\alpha * cos\theta + I_\beta * sin\theta \quad (1)$$

$$I_Q = -I_\alpha * sin\theta + I_\beta * cos\theta \quad (2)$$

This transformation converts vectors in 2-phase orthogonal stationary system into the rotating reference frame as shown in figure below:

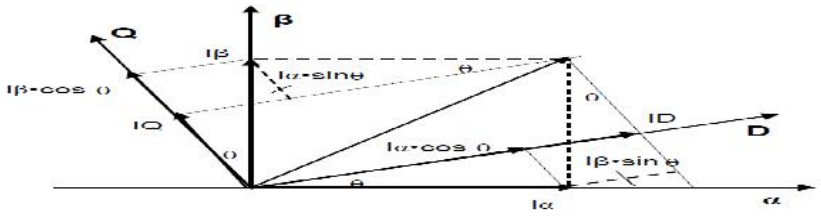

Figure 4. Park transform[19]

The instantaneous input quantities are defined by the following equations:

$$I_\alpha = I * \cos(\omega t) \quad (3)$$

$$I_\beta = I * \sin(\omega t) \quad (4)$$

Bidirectional DC to DC Converter

The DC/DC converter is used to provide a regulated dc voltage at higher level to the inverter and to control power flow to and from the motor during motoring and generating modes respectively. Generally DC/DC converter has some functions. These are convert a DC input voltage into a DC output voltage, regulate the DC output voltage against load and line variations, reduce the AC voltage ripple on the DC output voltage below the required level, provide isolation between the input source and the load if required and protect the supplied system and the input source from electromagnetic interference. The power converter for battery energy storage can be simply designed with a PWM converter with 3-phase transformer. This converter has simple structure and high efficiency, but the harmonic level of output current increases when the modulation index of PWM converter is low. So, the operation range of battery voltage is narrow, and the flexibility of current control is small [20][21]. In order to solve these weak points, a Bidirectional DC-DC converter was inserted between the 3-phase SVPWM inverter and the battery for this thesis. The DC-DC converter for charging and discharging the battery requires stable power control, highly efficient power conversion, and reliable power transfer regardless the voltage variation in battery. The insertion of DC-DC converter between the inverter and the battery can offer wider operation range and more flexible control.

The bidirectional dc-dc converter block controls the dc bus voltage and the charging and discharging current of the battery operates with a fixed duty ratio. The dc bus voltage is controlled using PI controller.

Phase Voltage Reconstruction

Description: This block calculates three phase voltages impressing to the 3-ph electric motor (i.e., induction) by using the conventional voltage-source inverter. Three phase voltages can be reconstructed from the DC-bus voltage and three switching functions of the upper power switching devices in the inverter. In addition, this block also includes the Clarke transformation changing from three phase voltages into two stationary dq-axis phase voltages.

The phase voltage of a general 3-ph motor (V_{an},V_{bn} andV_{cn}) can be calculated from the DC-bus voltage (V_{dc}) and three upper switching functions of inverter(S_1,S_2 andS_3)[19]. The 3-ph windings of motor are connected as the Y connection without a neutral return path (or 3-ph, 3-wire system). The overall system can be shown in Figure 5.

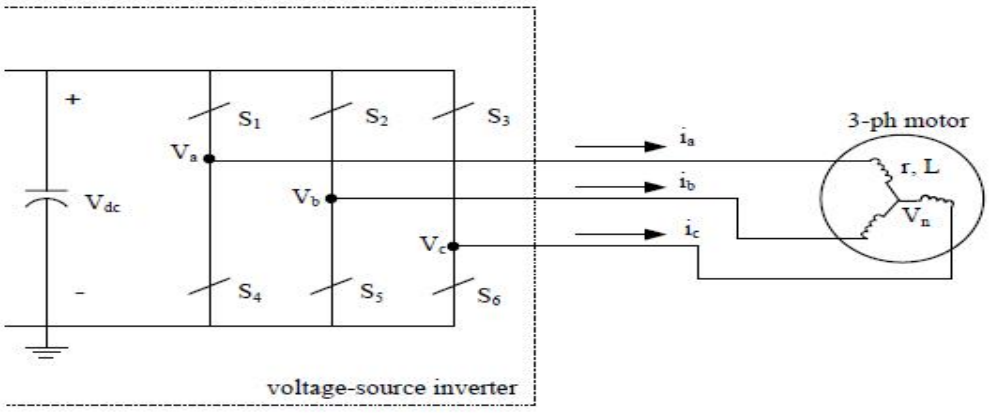

Figure 5: Voltage Source Inverter with 3-ph Electric Motor[19]

Each phase of the motor is simply modeled as a series impedance of resistance and inductance (r, L) and back emf (e_a,e_b, e_c). Thus, three phase voltages can be computed as:

$$V_{an} = V_a - V_n = i_a * r + L\frac{di_a}{dt} + e_a \quad (1)$$

$$V_{bn} = V_b - V_n = i_b * r + L\frac{di_b}{dt} + e_b \quad (2)$$

$$V_{cn} = V_c - V_n = i_c * r + L\frac{di_c}{dt} + e_c \quad (3)$$

Summing these three phase voltages, yields

$$V_a + V_b + V_c - 3V_n = (i_a + i_b + i_c)r + L\frac{d(i_a+i_b+i_c)}{dt} + e_a + e_b + e_c \quad (4)$$

Without a neutral return path, according to KCL, i.e. $i_a + i_b + i_c = 0$, and the back emfs are balanced and symmetrical due to the 3-ph winding structures, i.e.,

$e_a + e_b + e_c = 0$, so (4) becomes

$$V_{an} + V_{bn} + V_{cn} = 0 \tag{5}$$

Furthermore, the neutral voltage can be simply derived from Equation (4)-(5) as

$$V_n = \frac{1}{3}(V_a + V_b + V_c) \tag{6}$$

Now three phase voltages can be calculated as

$$V_{an} = V_a - \frac{1}{3}(V_a + V_b + V_c) = \frac{2}{3}V_a - \frac{1}{3}V_b - \frac{1}{3}V_c \tag{7}$$

$$V_{bn} = V_b - \frac{1}{3}(V_a + V_b + V_c) = \frac{2}{3}V_b - \frac{1}{3}V_a - \frac{1}{3}V_c \tag{8}$$

$$V_{cn} = V_c - \frac{1}{3}(V_a + V_b + V_c) = \frac{2}{3}V_c - \frac{1}{3}V_a - \frac{1}{3}V_b \tag{9}$$

Three voltages V_a,V_b, V_c are related to the DC-bus voltage (V_{dc}) and three upper switching functions (S_1, S_2, S_3) as the following relation

$$V_a = S_1 V_{dc} \tag{10}$$

$$V_b = S_2 V_{dc} \tag{11}$$

$$V_c = S_3 V_{dc} \tag{12}$$

Where S_1, S_2, S_3 = either 0 or 1, and S_4 = 1-S_1, S_5 = 1-S_2, and S_6 = 1-S_3. (13)

As a result, three phase voltages in Equation (7)-(9) can also be expressed in terms of DC-bus voltage and three upper switching functions as follows:

$$V_{an} = V_{dc}(\frac{2}{3}S_1 - \frac{1}{3}S_2 - \frac{1}{3}S_3) \tag{14}$$

$$V_{bn} = V_{dc}(\frac{2}{3}S_2 - \frac{1}{3}S_1 - \frac{1}{3}S_3) \tag{15}$$

$$V_{cn} = V_{dc}(\frac{2}{3}S_3 - \frac{1}{3}S_1 - \frac{1}{3}S_2) \tag{16}$$

It is emphasized that theS_1, S_2 and S_3 are defined as the upper switching functions. If the lower switching functions are available instead, then the out-of-phase correction of switching functions is required in order to get the upper switching functions as easily computed from Equation (13).

Next the Clarke transformation changing from three phase voltages (V_{an}, V_{bn}, and V_{cn}) to the stationary dq-axis phase voltages ($V_{ds}{}^{s}$ and $V_{qs}{}^{s}$) are applied by using the following relationship. Because of the balanced system in Equation (5), V_{cn} is not used in Clarke transformation

$$V_{ds}{}^{s} = V_{an} \tag{17}$$

$$V_{qs}{}^{s} = \frac{1}{\sqrt{3}}(V_{an} + 2V_{bn}) \tag{18}$$

Figure 6 depicts the abc-axis and stationary dq-axis components for the stator voltages of motor. Notice that the notation of the stationary dq-axis is sometimes used as the stationary αβ-axis, accordingly.

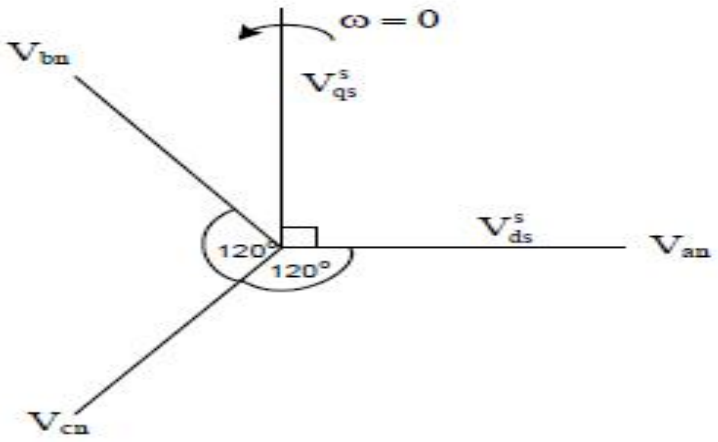

Figure 6: The abc-axis and Stationary dq-axis Components of The Stator Phase Voltages

2.6PI Controller

Description: This block implements a simple PI controller with anti-windup correction.

The PI block implements a basic summing junction and P+I control law with the following features:

- Programmable output saturation
- Independent reference weighting on proportional path
- Anti-windup integrator reset

The PI controller is a sub-set of the PID controller. A block diagram of the internal controller structure is shown below.

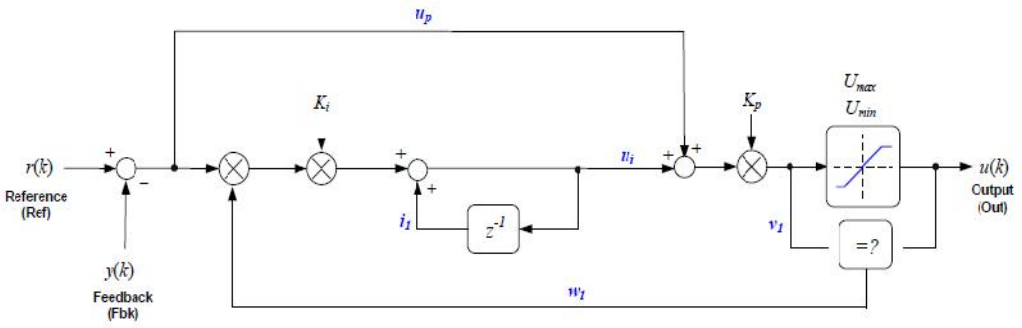

Figure 7: PI Controller [19]

a) Proportional path

The proportional path is a direct connection between the error term and a summing junction with the integral path. The error term is:

$$e(k)= r(k) - y(k) \quad (1)$$

Proportional gain is applied to the sum of proportional and integral paths, as described in section c).

b) Integral path

The integral path consists of a discrete integrator which is pre-multiplied by a term derived from the output module. The term w1 is either zero or one, and provides a means to disable the integrator path when output saturation occurs. This prevents the integral term from "winding up" and improves the response time on recovery from saturation. The integrator law used is based on a backwards approximation

$$u_i(K) = u_i(k-1) + K_i[r(k) - y(k)] \quad (2)$$

c) Output path

The output path contains a multiplying term (K_p) which acts on the sum of the proportional and integral controller terms. The result is then saturated according to user programmable upper and lower limits to give the controller output.

The pre-and post-saturated terms are compared to determine whether saturation has occurred, and if so, a zero or one result is produced which is used to disable the integral path (see above). The output path law is defined as follows.

$$V_1(k) = K_p[u_p(k) + u_i(k)] \tag{3}$$

$$U(k) = \begin{cases} U_{max} : V_1(k) > U_{max} \\ U_{min} : V_1(k) < U_{min} \\ V_1(k) : U_{min} < V_1(k) < U_{max} \end{cases} \tag{4}$$

$$w_1(k) = \begin{cases} 0 : V_1(k) \neq U(k) \\ 1 : V_1(k) = U(k) \end{cases} \tag{5}$$

Tuning the P+I controller

A suggested general technique for tuning the controller is now described.

Step 1: Ensure integral is set to zero and proportional gain set to one.

Step 2: Gradually adjust proportional gain variable (K_p) while observing the step response to achieve optimum rise time and overshoot compromise.

Step 3: If necessary, gradually increase integral gain (K_i) to optimize the return of the steady state output to nominal. The controller will be very sensitive to this term and may become unstable so be sure to start with a very small number. Integral gain will result in an increase in overshoot and oscillation, so it may be necessary to slightly decrease the $K_p$term again to find the best balance. Note that if the integral gain is used then set to zero, a small residual term may persist inu_i.

2.7 Space Vector Pulse Width Modulation

*Description:*This block calculates the appropriate duty ratios needed to generate a given stator reference voltage using space vector PWM technique. The stator reference voltage is described by its (α,β) components, Ualpha and Ubeta.

Discontinuous Space Vector generator

*Description:*This block calculates the appropriate duty ratios needed to generate a given stator reference voltage using space vector PWM technique. The stator reference voltage is described by its (α,β) components, Ualpha and Ubeta. Different than the regular SVGEN, this modulation technique keeps one of the three switches off during the entire 120^0 to minimize switching losses. This technique is also known as DPWMmin in the literature [19].

The Space Vector Pulse Width Modulation (SVPWM) refers to a special switching sequence of the upper three power devices of a three-phase voltage source inverters (VSI) used in application such as AC induction and permanent magnet synchronous motor drives. This special switching scheme for the power devices results in 3 pseudo-sinusoidal currents in the stator phases.

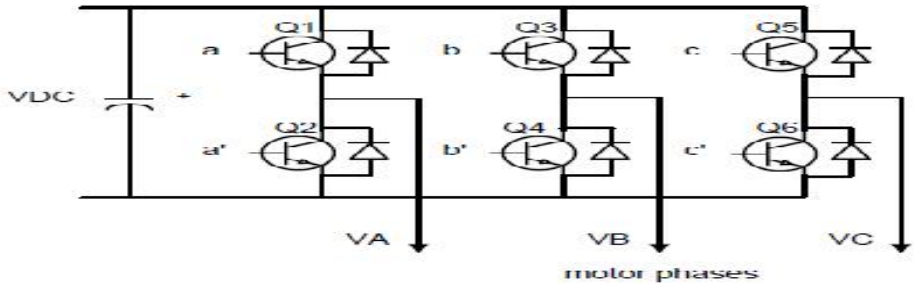

Figure8. Power circuit topology for a three-phase VSI [19]

It has been shown that SVPWM generates less harmonic distortion in the output voltages or currents in the windings of the motor load and provides more efficient use of DC supply voltage, in comparison to direct sinusoidal modulation technique.

For the three phase power circuit topology configurations shown in Figure 8 there are eight possible combinations of on and off states of the upper power transistors.

These combinations and the resulting instantaneous output line-to-line and phase voltages, for a dc bus voltage of V_{dc}, are shown in Table 1.

Table 1: Device on/off patterns and resulting instantaneous voltages of a 3-phase power inverter

C	B	A	V_{AN}	V_{BN}	V_{CN}	V_{AB}	V_{BC}	V_{CA}
0	0	0	0	0	0	0	0	0
0	0	1	$2\frac{V_{dc}}{3}$	$-\frac{V_{dc}}{3}$	$-\frac{V_{dc}}{3}$	V_{dc}	0	$-V_{dc}$
0	1	0	$-\frac{V_{dc}}{3}$	$2\frac{V_{dc}}{3}$	$-\frac{V_{dc}}{3}$	$-V_{dc}$	V_{dc}	0
0	1	1	$\frac{2V_{dc}}{3}$	$\frac{V_{dc}}{3}$	$-2\frac{V_{dc}}{3}$	0	$2V_{dc}$	$-V_{dc}$
1	0	0	$-\frac{2V_{dc}}{3}$	$-\frac{V_{dc}}{3}$	$2\frac{V_{dc}}{3}$	0	$-V_{dc}$	V_{dc}
1	0	1	$\frac{V_{dc}}{3}$	$-2\frac{V_{dc}}{3}$	$\frac{V_{dc}}{3}$	V_{dc}	$-V_{dc}$	0
1	1	0	$-\frac{V_{dc}}{3}$	$\frac{2V_{dc}}{3}$	$-\frac{V_{dc}}{3}$	$-V_{dc}$	0	V_{dc}
1	1	1	0	0	0	0	0	0

The quadrature quantities (in d-q frame) corresponding to these 3 phase voltages are given by the general Clarke transform equation:

$$V_{ds} = V_{AN} \tag{1}$$

$$V_{qs} = \frac{2V_{BN}+V_{AN}}{\sqrt{3}} \tag{2}$$

In matrix from the above equation is also expressed as,

$$\begin{bmatrix} V_{ds} \\ V_{qs} \end{bmatrix} = \frac{2}{3}\begin{bmatrix} 1 & -\frac{1}{2} & -\frac{1}{2} \\ 0 & \frac{\sqrt{3}}{2} & -\frac{\sqrt{3}}{2} \end{bmatrix}\begin{bmatrix} V_{AN} \\ V_{BN} \\ V_{CN} \end{bmatrix} \tag{3}$$

Due to the fact that only 8 combinations are possible for the power switches, V_{ds} and V_{qs} can also take only a finite number of values in the (d-q) frame according to the status of the transistor command signals (c,b,a). These values of V_{ds} and V_{qs} for the corresponding instantaneous values of the phase voltages (V_{AN}, V_{BN}, V_{CN}) are listed in Table 2.

Table2: Switching patterns, corresponding space vectors and their (d-q) components

C	B	a			Vector
0	0	0	0	0	
0	0	1	-2	0	
0	1	0	−		
0	1	1			
1	0	0	−	−	
1	0	1		−	
1	1	0	2	0	
1	1	1	0	0	

These values of V_{ds} andV_{qs}, listed in Table 2, are called the (d-q) components of the basic space vectors corresponding to the appropriate transistor command signal (c, b, a). The space vectors corresponding to the signal (c, b, a) are listed in the last column in Table 2. For example, (c, b, a) =001 indicates that the space vector is U0.The eight basic space vectors defined by the combination of the switches are also shown in Figure9 [19][22].

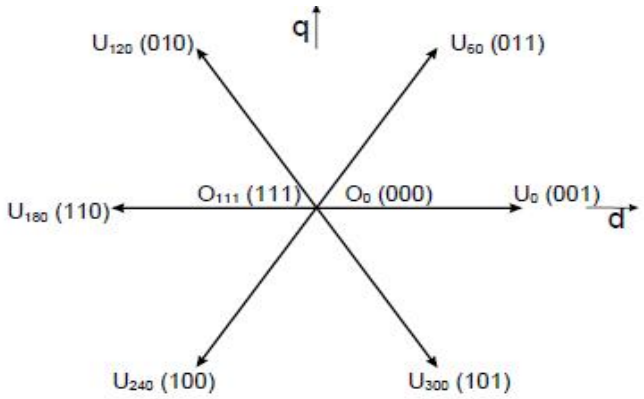

Figure9: Basic Space Vectors

In Figure 9, vectors corresponding to states 0 (000) and 7 (111) of the switching variables are called the zero vectors.

Space Vector PWM can be implemented by the following steps:

Step 1: DetermineV_d,V_q, V_{ref}, and angle (theta)

Step 2: Determine Sector

Step 3: Determine time duration T1, T2, T0

Step 4: Determine the switching time of each switch (S1 to S6)

Step1: DetermineV_d, V_q, V_{ref} and Angle(theta)

$$V_d = V_{an} - V_{bn}\cos 60 - V_{cn}\cos 60 \quad (4)$$

$$V_q = 0 + V_{bn}\cos 30 - V_{cn}\cos 30 \quad (5)$$

$$V_d = V_{an} - \frac{V_{bn}}{2} - \frac{V_{cn}}{2} \quad (6)$$

$$V_q = \frac{\sqrt{3}}{2}V_{bn} - \frac{\sqrt{3}}{2}V_{cn}, \begin{bmatrix} V_d \\ V_q \end{bmatrix} = \frac{2}{3}\begin{bmatrix} 1 & \frac{-1}{2} & \frac{-1}{2} \\ 0 & \frac{\sqrt{3}}{2} & -\frac{\sqrt{3}}{2} \end{bmatrix}\begin{bmatrix} V_{an} \\ V_{bn} \\ V_{cn} \end{bmatrix} \quad (7)$$

Magnitude$\left|V_{ref}\right| = \sqrt{{V_d}^2 + {V_q}^2}$ (8)

Angle$theta = \tan^{-1}(\frac{V_q}{V_d})$ (9)

Step2: Determine Sector

Table 3: Determining Sectors

Angle(θ)	Sector where V_{ref} is placed
$0^{o} \leq \theta < 60^{o}$	Sector 1
$60^{o} \leq \theta < 120^{o}$	Sector 2
$120^{o} \leq \theta < 180^{o}$	Sector 3
$120^{o} \leq \theta < 180^{o}$ $-180^{o} \leq \theta < -120^{o}$	Sector 4
$-120^{o} \leq \theta < -60^{o}$	Sector 5
$-60^{o} \leq \theta < 0^{o}$	Sector 6

Step3: Determine Time Duration T_1, T_2, T_0

The general formula for calculating switching time duration at any sector

$$T_1 = \frac{\sqrt{3}T_s|V_{ref}|}{V_{dc}}\left(\sin\left(\frac{n\Pi}{3}\cos\alpha - \cos\frac{n\Pi}{3}\sin\alpha\right)\right) \quad (10)$$

$$T_2 = \frac{\sqrt{3}T_s|V_{ref}|}{V_{dc}}\left(-\cos\alpha\sin\left(\frac{n-1}{3}\Pi + \sin\alpha\cos\frac{n-1}{3}\Pi\right)\right) \quad (11)$$

$$T_0 = T_s - T_1 - T_2 \quad (12)$$

Step4: Determine the Switching Time of Each Switch

This step determines the switching time of each switch at each sector called delay [23].

Chapter Three
Regenerative Braking Analysis of Induction Motor

3.1 Different Braking Methods

Basically the methods of electrical braking include regenerative braking, plug braking and Dynamic Braking. Dynamic braking is similar to regenerative braking, but instead of storing energy, it is dissipated on a resistance. Dynamic braking can be applied in any speed, regardless of boosting. But, a limitation occurs when speed of the system is relatively low and required braking torque is high. Even if the system is short circuited (brake resistance is zero), heavy systems or systems with high moment of inertia cannot be stopped quickly.

Plugging is a method, which is used in heavy systems with very high inertia and should be stopped quickly. Different from the previous electrical braking systems, both voltage and current are reversed in plugging (by reversing phase sequence), resulting consumption of energy to stop the system. In plug braking, back EMF and line voltage is in the same direction, resulting very high braking current and torque. While designing a system with plug braking, one should consider high current would be flowing on electronic components and all of the active components should be sized and cooled accordingly. Also, since this system consumes energy to brake, it would be costly to operate. So, this type of braking should be used with other electrical braking methods [24].

In regenerative braking the main idea is to save the energy. Kinetic energy of the moving or rotating system is turned back into electrical energy. For battery powered systems, like electrical vehicles, regenerated energy is saved on the batteries. For line-fed systems, it can be sent back to the line to feed another motor connected to the line. Regenerative braking needs generator operation of electric machine. In this respect, current and voltage is reversed with respect to each other. Voltage is positive to motion but current is from the system to the source, which is the opposite of what happens in motor mode. Regenerative braking and plug braking are widely used because regenerative braking is known for its braking energy efficiency and plug braking is known for its braking time efficiency[24][25].Plug braking can be obtained by reversing the

phase of any two terminals out of the 3Φ supply terminals of the IM. With the reversal of terminals, the torque also reverses which opposes the normal operation of the machine and reduces the speed of the vehicle and thus braking is obtained. The regenerative braking is obtained by driving the rotor with a negative slip. With the slip being negative, the machine operates as a generator and the load supplies power to the source, thereby the direction of current and torque reverses which causes braking in the drive [24][25][26][27][28].

Although mechanical braking method is an efficient method of instantaneous braking, but there is no restoration of energy in the process. The entire energy is wasted as thermal energy. Hence, as a suitable alternative, regenerative braking has been introduced. Although the effectiveness of braking in terms of fastness has been decreased with regenerative braking in comparison to plugging but the restoration of power and energy during braking into the battery makes it more efficient for vehicle dynamics.

3.2Energy Balance of overall system

Regenerative braking is a motor operating mode, where the mechanical power (stored as kinetic energy) of the motor and coupled driving unit is converted to electrical energy and fed back to the electric system[14]. The overall block diagram of the power analysis during regenerative braking is shown in the figure10. To analyze the power during braking the following are considered:

3.2.1 Rate of change of kinetic energy:

$$P_{KE} = \frac{d}{dt}(KineticEnergy) \tag{1}$$

Kinetic energy due to rotational motion can be formulated as:

$$KE = \frac{1}{2}Jw^2 \tag{2}$$

Therefore power due to rotational motion can be

$$P_{KE} = J\frac{dw}{dt}w \tag{3}$$

Since the system is a nonlinear system, kinetic energy due to linear motion can be neglected.

3.2.2 *Mechanical power loss:* There are two mechanical power losses from the available kinetic energy before it is converted to electrical power. These are frictional loss and loss due to load. But in this thesis no load condition is considered. Therefore the power loss due to the load can be neglected.

$$P_{mloss} = Bw^2 \tag{4}$$

3.2.3 *Electrical power:* the remaining mechanical power to be converted to electrical power is then:

$$P_{KE} - P_{mloss} = P_{eloss} + P_{feedback} \tag{5}$$

3.2.4 *Electrical power loss in the machine:* when the electric machine operates as electric generator there is electrical power loss, which can be divided into core loss and copper losses. This loss can be analyzed as conventional generator losses. Furthermore, there is power loss in the power processing units. Let the electrical loss in machine and power processor be represented as P_{eloss}

$$P_{eloss} = coreloss + coperloss \tag{6}$$

But in this analysis all electrical losses are neglected.

Therefore the overall power balances with P_{fb} as power which can be feed back to the electric power system is given by:

$$P_{feedback} = P_{KE} - P_{mloss} \tag{7}$$

$$P_{feedback} = J\frac{dw}{dt}w - Bw^2 \tag{8}$$

From the power electronics circuit, power on the ac side can be:

$$P_{ACside} = \frac{3}{2}(V_{qs} * i_{qs} + V_{ds} * i_{ds}) \tag{9}$$

Power on the dc side comes from power of the battery.

Based on the above description the electrical power, mechanical power and battery power balance have been analyzed to see the overall power in the system during regenerative braking.

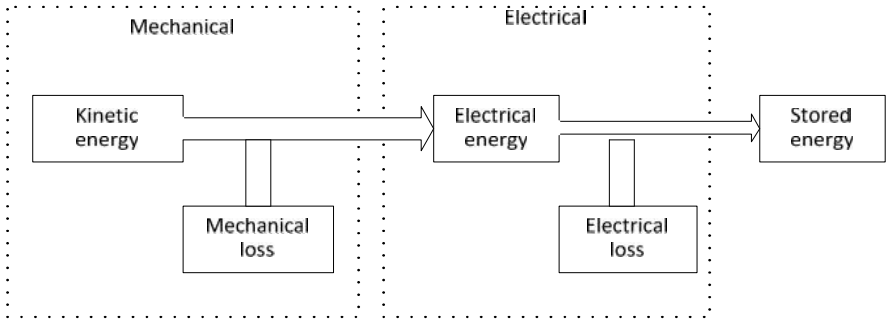

Figure 10: Power Analysis during Regenerative Braking

Chapter Four
Simulation and Experimental Results

4.1 Overall System Analysis

The brief description of the overall regenerative braking system is in figure 11 for a system overview. The regenerative braking system in this thesis includes an induction motor, a three phase inverter, a bidirectional dc/dc converter, a battery, a speed and flux estimation mechanism and a control system. The speed, the torque and flux of IM is controlled by three anti windup PI controllers. The battery system mathematical model was derived. Based on the battery power, the dc and ac side of inverter power calculation and analysis has been done. The battery state of charge, current and voltage are analyzed during regenerative braking and the power system analysis is done by comparing the mechanical power obtained from the motor, the electrical power generated by the motor acts as generator during regenerative braking and the battery power. The regenerative braking is designed by controlling motor Torque using anti windup controller for running the motor with negative slip.

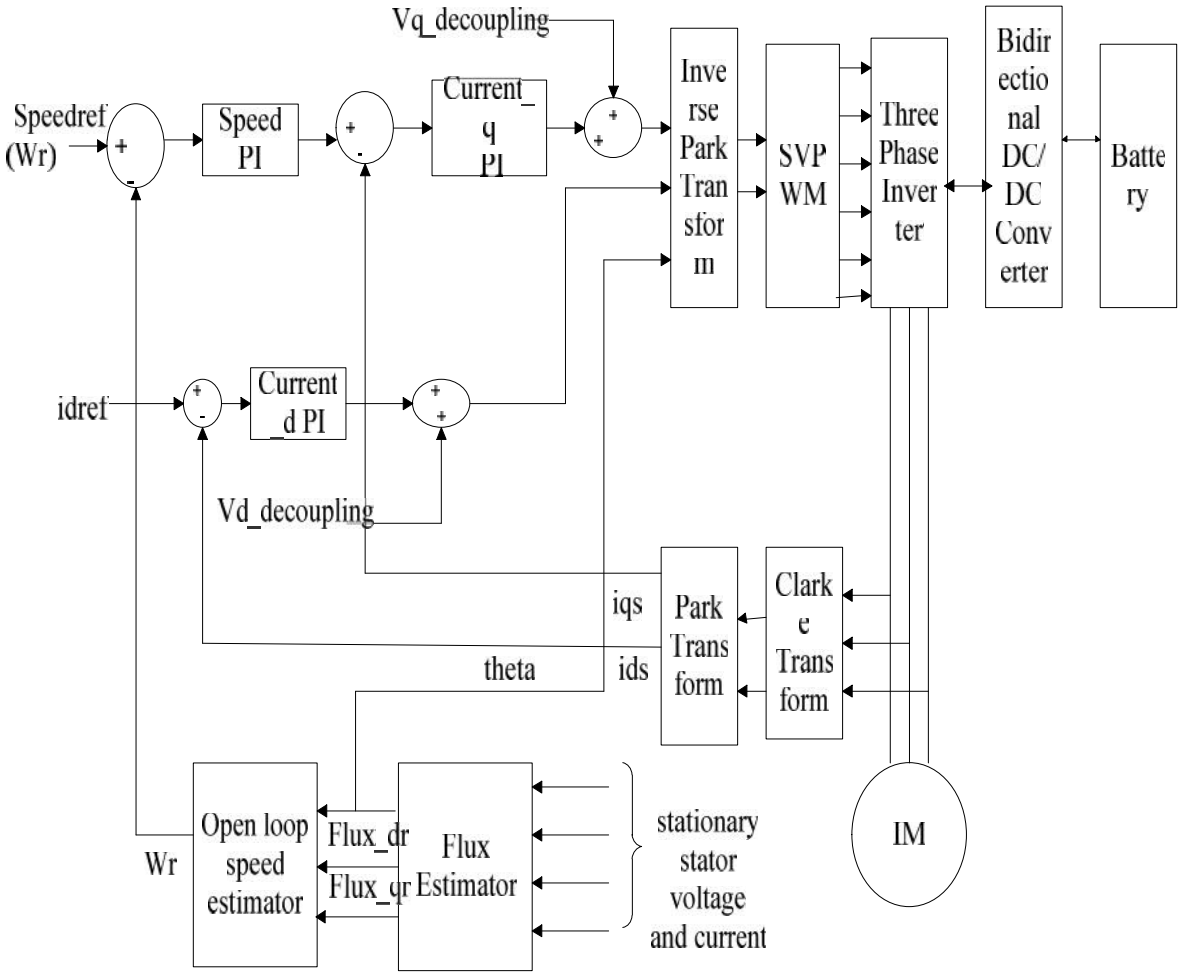

Figure 11Overall System Block Diagram

The bidirectional dc/dc converter is a basic circuit in regenerative braking system. During motoring mode the motor is fed by the battery voltage boosted by the dc/dc converter to get the necessary dc bus voltage for the motor to run. During braking the motor acts as generator to convert the kinetic energy to electrical energy and fed back to the low voltage battery by bucking the dc bus voltage using the dc/dc converter.

Sensors mounted on the machine shaft are in general not desirable for a number of reasons. First of all, their cost is substantial. Secondly, their mounting requires a machine with two shaft ends available - one for the sensor, and the other one for the load coupling. Thirdly, electrical signals from the shaft sensor have to be taken to the controller and the sensor needs a power supply, and these require additional cabling. Finally, presence of a shaft sensor reduces mechanical

robustness of the machine and decreases its reliability. It is for all these reasons that substantial efforts have been put in recent past into possibilities of eliminating the shaft mounted sensor for rotor speed sensing. However, the information regarding actual speed and/or position of the rotor shaft remains to be necessary for closed loop speed (and/or) position control (and coordinate transformation, if applicable) even if the shaft sensor is not installed. Hence the speed (and/or position) has to be estimated somehow; from easily measurable electrical quantities (in general, stator voltages and currents).

The flux estimation technique is based on both current and voltage model as shown in figure 12. It can be seen the rotor flux linkage is calculated from the stator flux linkage. The stator flux linkage is produced by using pure integrator. To reduce the errors due to pure integrator and stator resistance measurement, the compensated voltages produced by PI compensators are introduced. Therefore, this flux estimator can be operating over a wide range of speed, even at very low speed (10% of rated speed). But this results in low performance in speeds below 10%of rated speed.

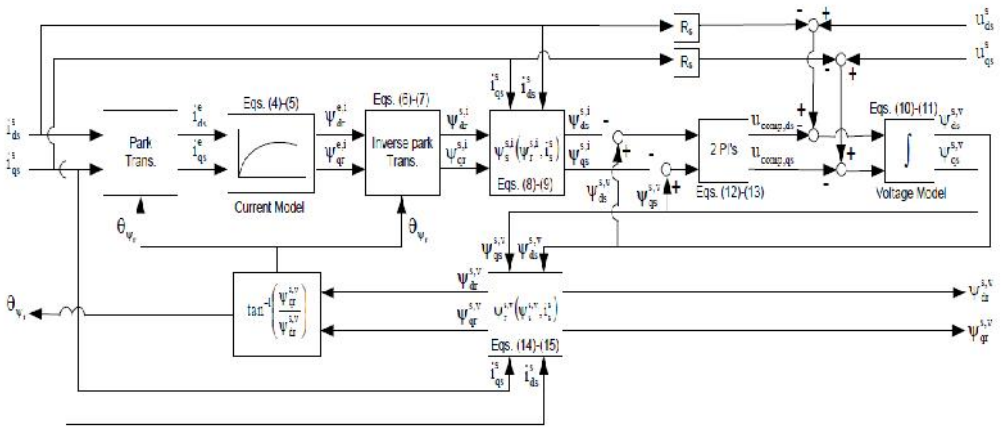

.

Figure 12 Overall System of Flux Estimator

The open loop speed estimation technique which is used in this thesis uses the rotor fluxes and position estimated in flux estimation technique. The open loop calculation method is simple to implement but prone to error because of high dependency on the machine parameters. In open loop estimator, especially at low speeds, parameters variation has significant influence on the performance of the drive both at steady state and transient state. The need for the derivation

makes this method more susceptible to noise. At low speeds the accuracy of this estimator is limited. The problems encountered in the implementation of this scheme are two-fold. Firstly, since it is model based, accuracy of speed estimation is affected by parameter variation effects. Secondly, the scheme involves pure integration that fails at very low and zero frequency due to offset and drifts problems. This kind of speed estimator works without failure above 10% of rated synchronous speed.

Regenerative braking mode can be achieved by driving the machine with negative slip, by the use of variable frequency drives. The process of regeneration also requires developing the desired braking torque as commanded by the driver. During transient conditions like braking in vehicles, vector control of IM gives proper torque control. Hence field oriented control (FOC) algorithm has been used.

In field oriented control algorithm the torque will be maximized when the current vector is defined orthogonal to the surface of the flux produced. The d-axis current control the flux of the IM and the q-axis current controls the electromagnetic torque. Hence by giving a negative torque command and ensuring that the direction of w_e is not negative, the machine is bound to operate in regenerative braking mode with maximum braking torque. This technique has been used to implement braking analysis in this thesis work.

The torque command is developed in accordance with the speed command using an anti-windup speed regulation controller. The feedback integration of the anti-windup prevents the integrator from integrating speed error beyond the maximum and minimum values of the torque command.

The torque and flux commands are regulated using PI controller into consideration of the current commands to develop the required voltage commands. These voltages are transformed to a stationary reference frame and fed to SVPWM. The inverter gates its gate signal from SVPWM and connected to battery through bidirectional converters.

The overall Simulink block diagram is shown below.

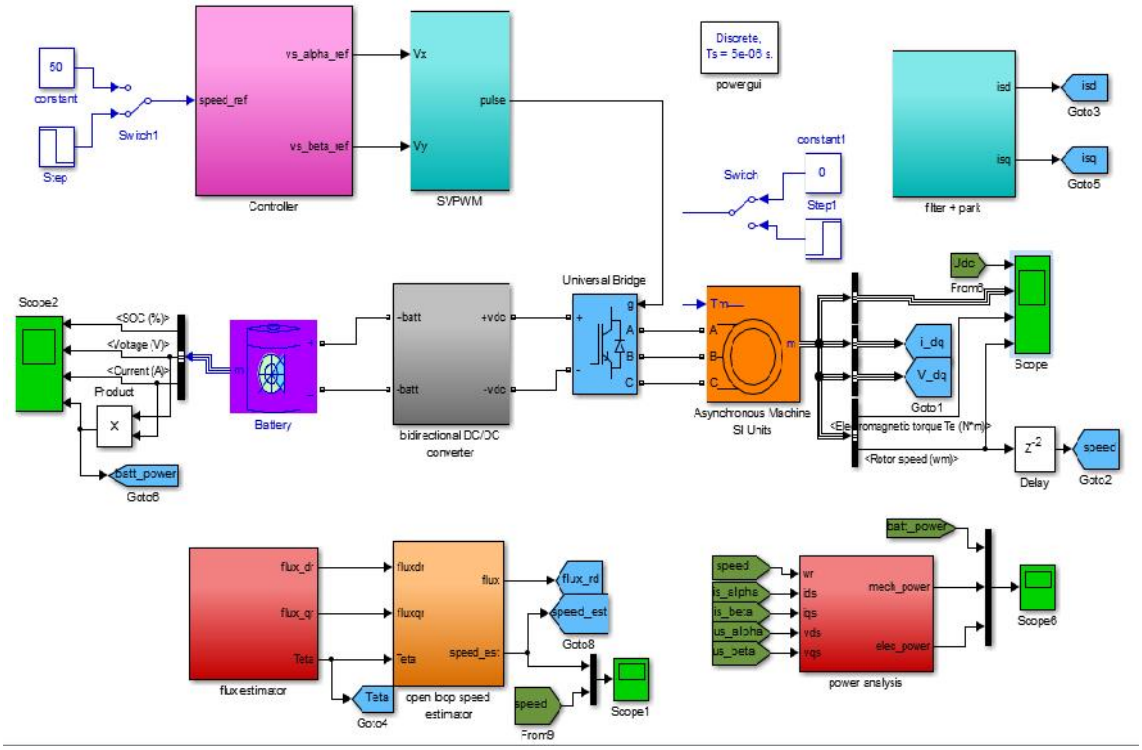

Figure13 Simulink Model of Overall System

The simulink model is developed using components from Simulink Power System block set. The induction motor used in this thesis simulation is 3-ϕ, 380-V, 2.2-KW, 50-Hz, 4-pole squirrel cage induction motor with parameters given in Table 4.

Table 4: Induction Motor and Control Parameters for Simulation and Experimentation:

Parameters	**Value**
Rated Power	2200 watt
Rated Voltage	380 Volt
Stator Resistance	2.76 Ohms
Stator Inductance	11.8e-03 Hertz
Rotor Resistance	3.11 Ohms
Rotor Inductance	11.8e-03 Hertz
Mutual Inductance	188.2e-3 Hertz
Moment of Inertia J	0.3
Viscous Friction B	0.01

No of pole pairs, P					2						
Frequency f					50 Hertz						
K	K	K	K	K	K	K	K	K	K	PWM freq	K
15	250	234	1765	4	496	18	200	1.5	0.5	5K	15

Parameters	**Value**
Rated Power	180Watt
Rated Voltage	236Volt
Stator Resistance	11.05 Ohms
Stator Inductance	0.316423 Hertz
Rotor Resistance	6.11 Ohms
Rotor Inductance	0.316423 Hertz
Mutual Inductance	0.293939 Hertz
No of pole pairs P	2

The proposed scheme is simulated in discrete time. The induction motor and inverter blocks used in the design are already available in the standard Simulink library. The blocks that had to be constructed were the open loop speed and flux estimator, bidirectional dc/dc converter block and direct field oriented control block as shown in figure 14, 15,16 and 17. The open loop based speed estimator calculates the rotor speed used in direct field oriented control which controls SVPWM that used to drive the voltage source inverter.

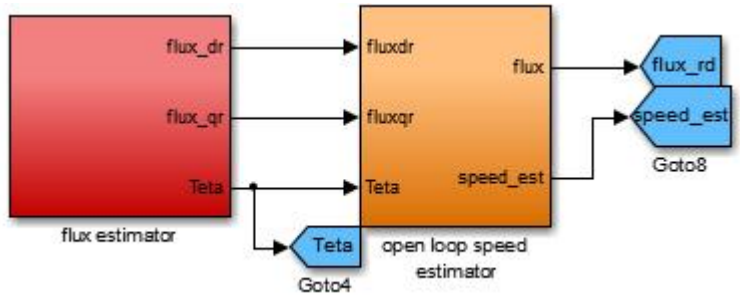

Figure 14 Flux and Speed Estimator

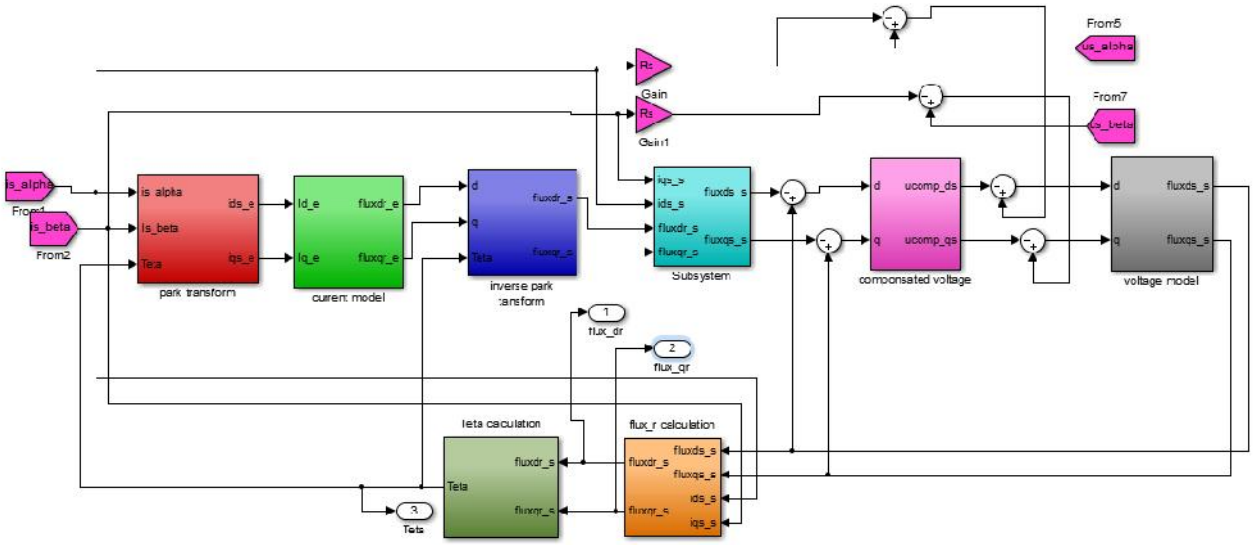

Figure 15 Voltage and Current model based Flux Estimation

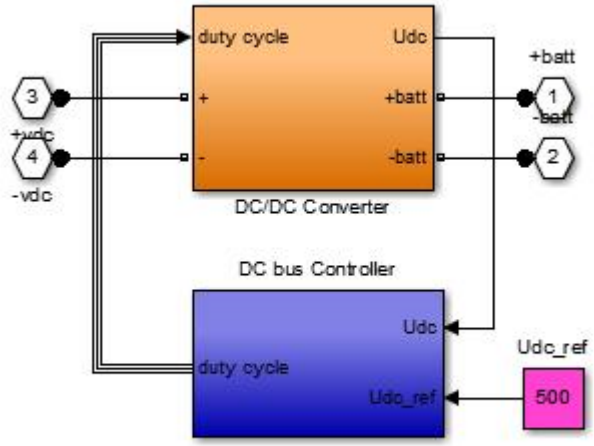

Figure 16 :Bidirectional dc/dc Converter

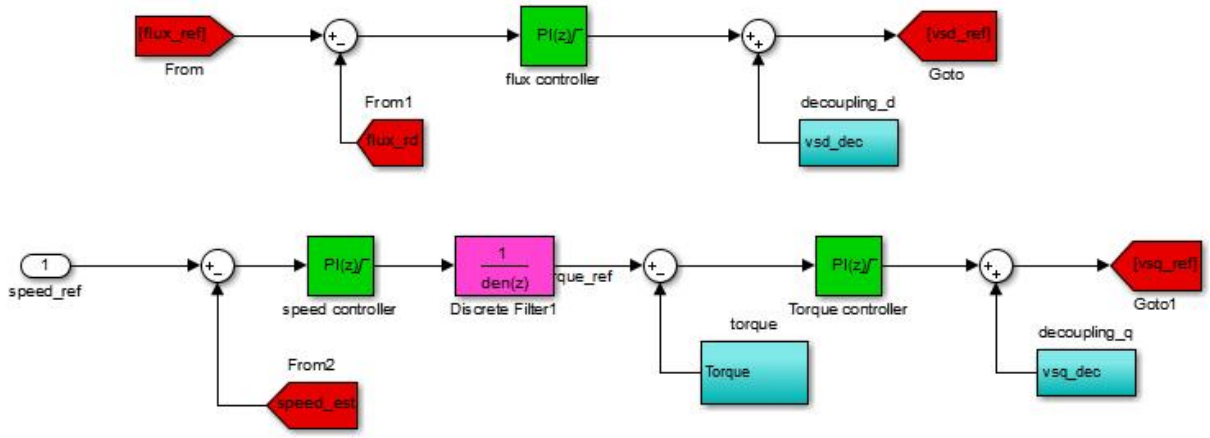

Figure 17 Direct field oriented control

4.2 Result and Discussion

The machine initially at rest is driven by a commanded speed speed* as shown in the figure13.The machine accelerates with speed w_r and therein at t=1s, the regenerative braking is initiated. As it is seen in the figure 18, with regenerative braking, the rate of deceleration decreases at low speeds than at high speeds. It takes more than 1s at low speeds which shows regenerative braking is inefficient at low speeds.

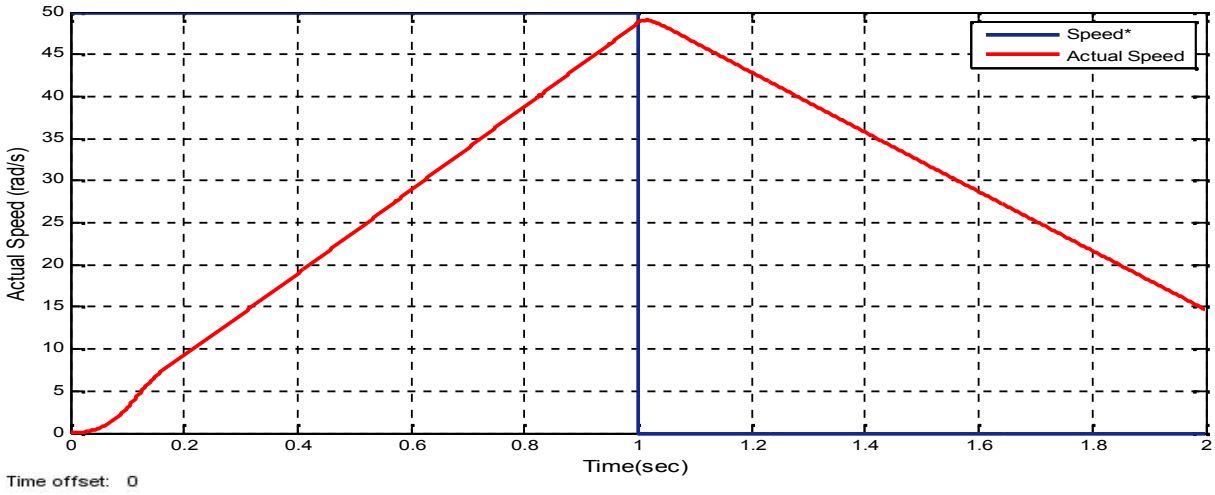

Figure18 Variation of Motor Actual Speed with Regenerative Braking

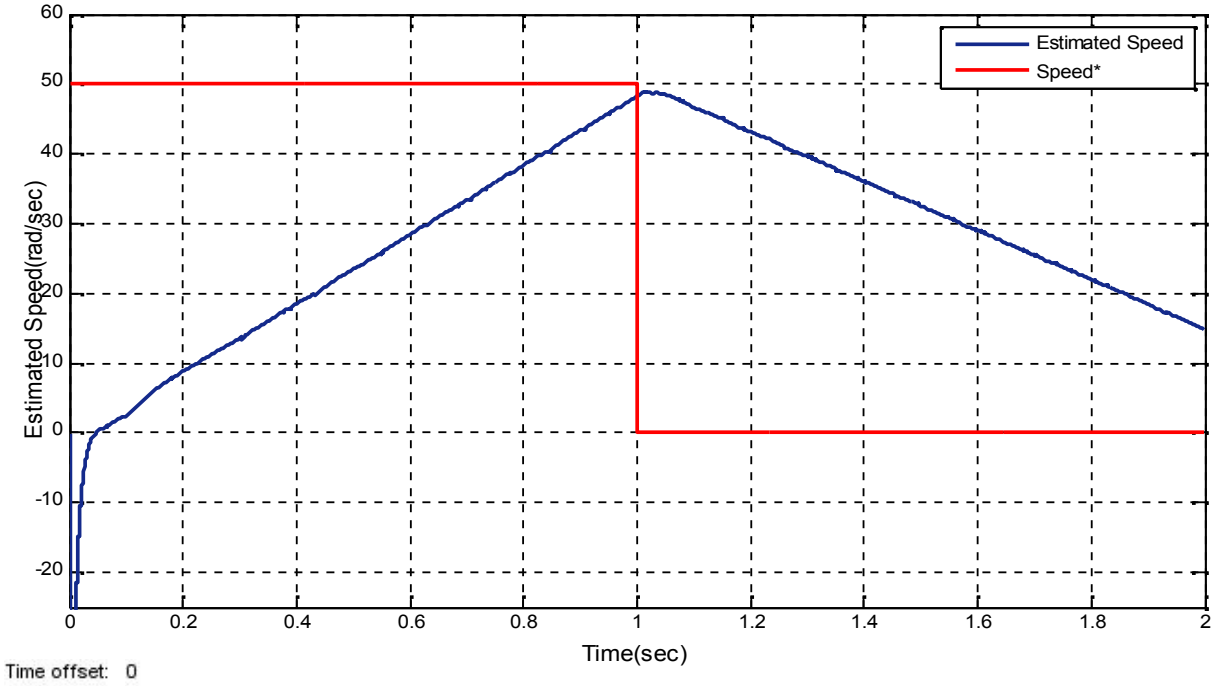

Figure 19Variation of Motor Estimated Speed with Regenerative Braking

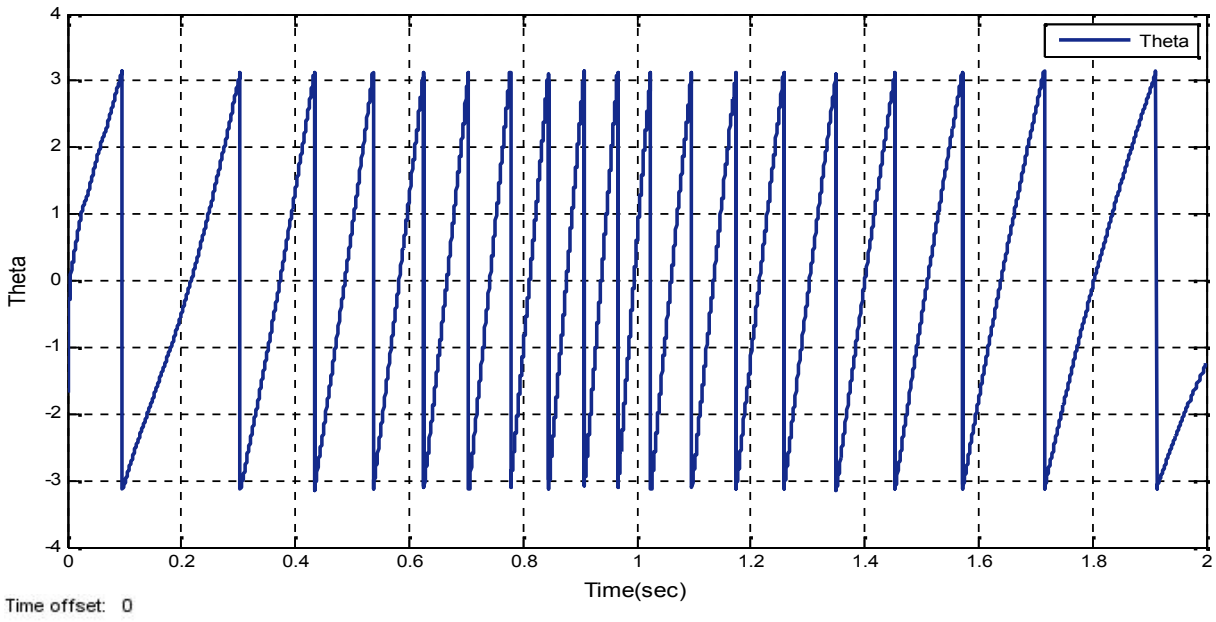

Figure 20Estimated Rotor Angle (theta)

The speed and rotor position are estimated in this thesis as shown in figure 19and 20. In figure19the speed estimated using open loop speed estimator has some ripple at time 0 to 0.2 second due to pure integrator in voltage model of rotor flux estimation and differentiator in open

loop speed estimation. This ripple results in change in the graphs of the other results in the given time interval in motoring mode.

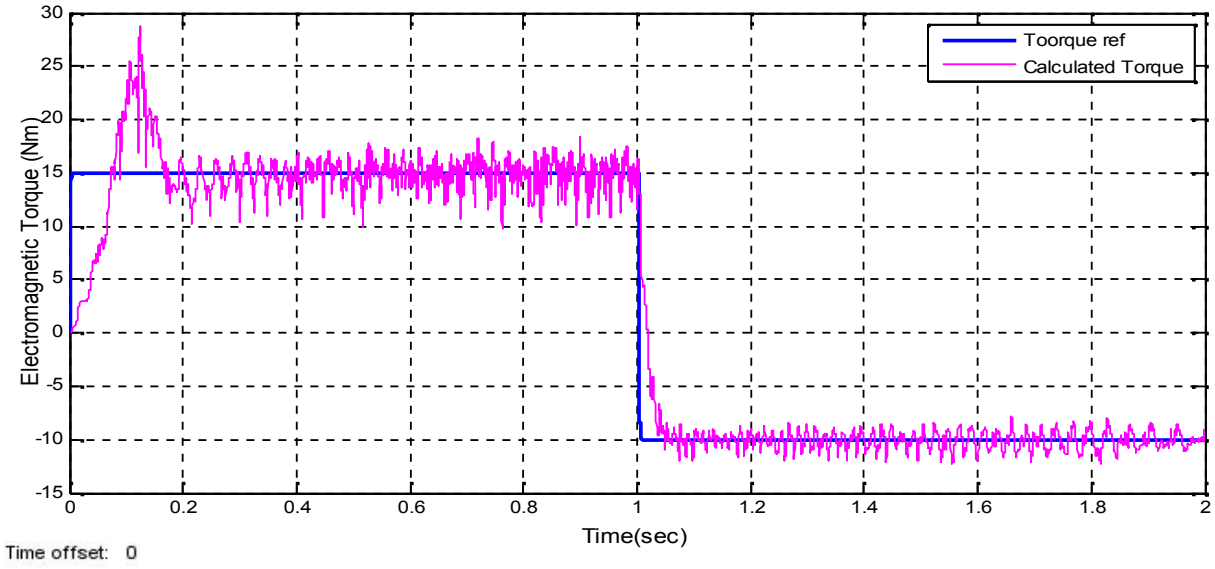

Figure 21: Variation of Motor Torque with Regenerative Braking

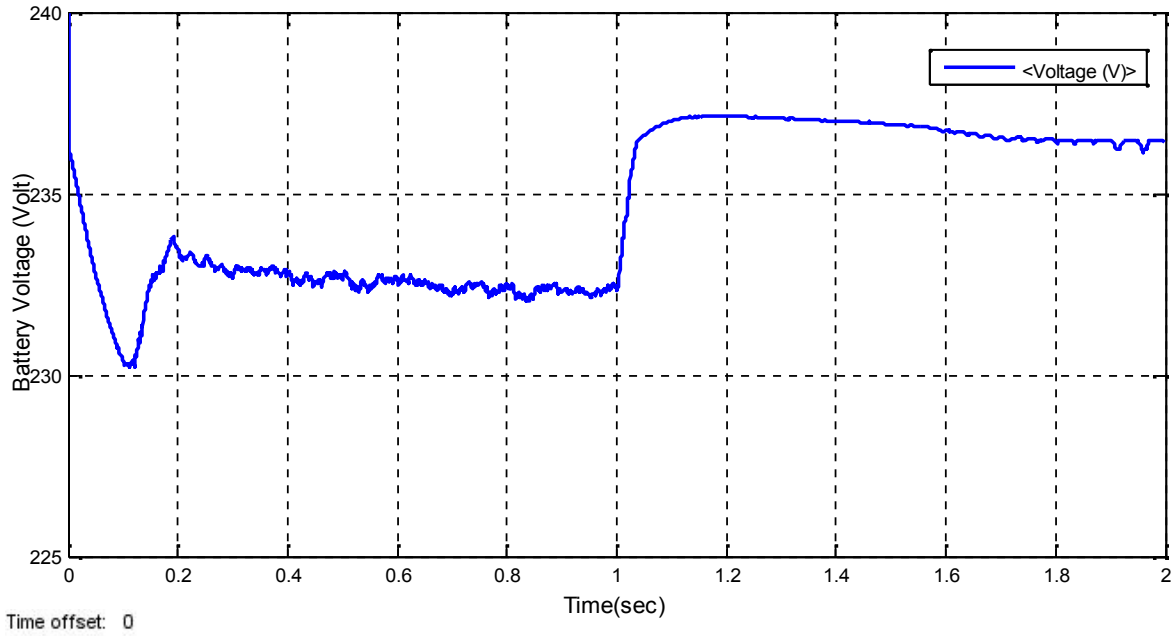

Figure22: Variation of Battery Voltage with Regenerative Braking

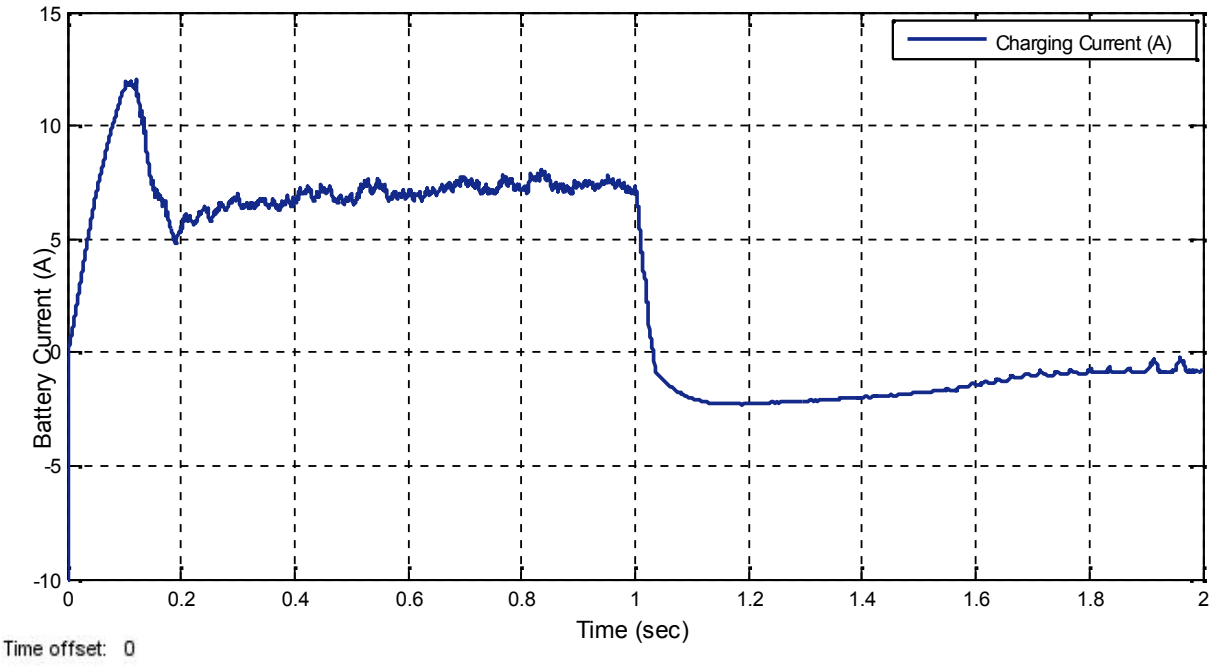

Figure 23: Variation of Battery Current with Regenerative Braking

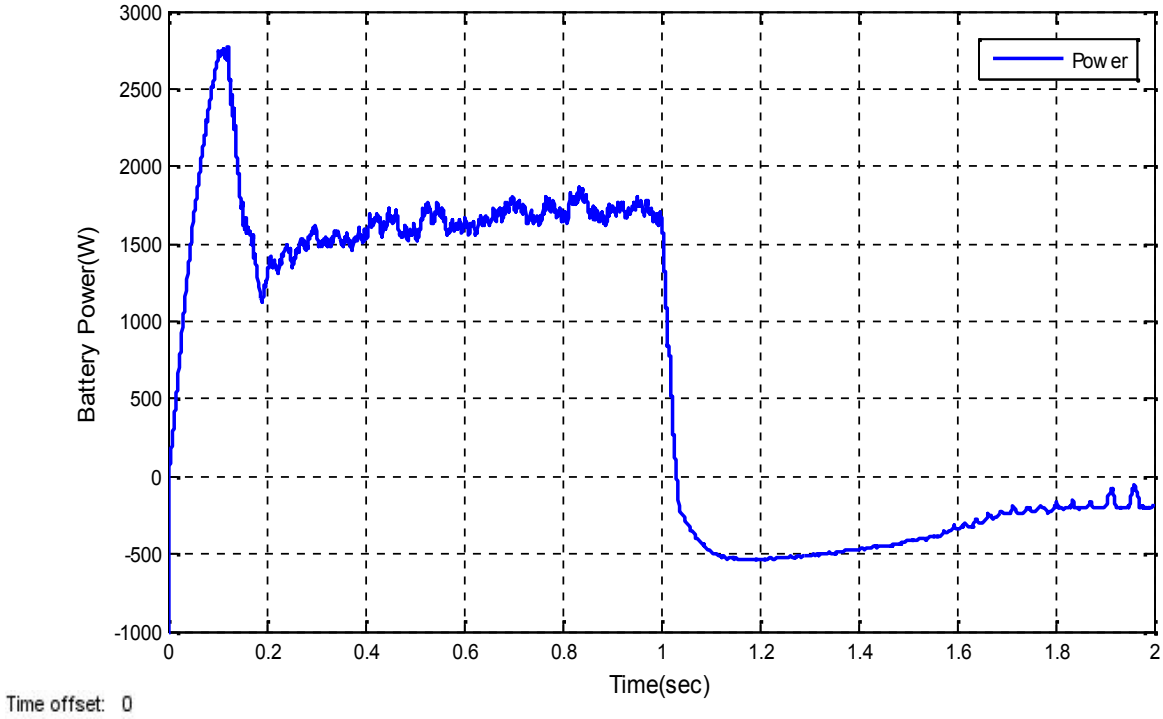

Figure 24: Variation of Battery Power with Regenerative Braking

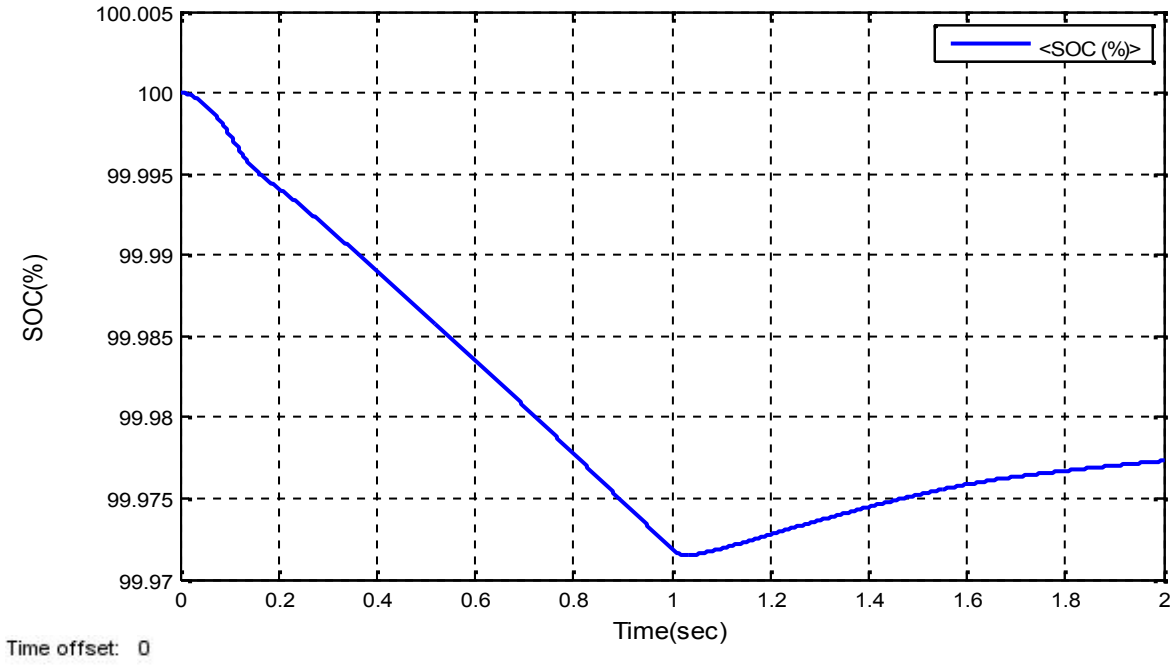

Figure 25: Variation of SOC of Battery with Regenerative Braking

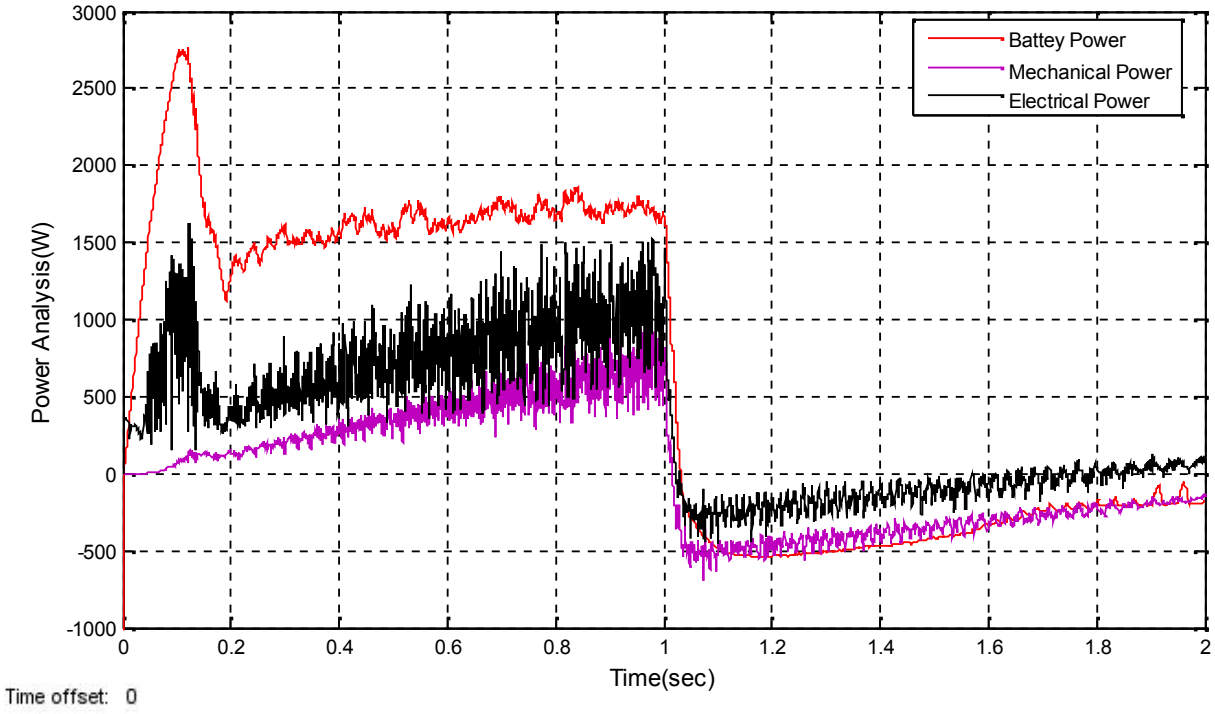

Figure 26Energy Balance during regenerative braking

The machine torque during braking attains a negative value of 10 N-m which can be used as braking torque shown in figure21. In figure 22, the battery voltage increases from its nominal voltage and the voltage remains positive throughout. The battery voltage is regenerated more than 50% of the lost voltage during motoring mode. The machine supplies power to the battery during braking in figure 24 which is around 500W is represented by the decrease of the battery current to negative values in figure 23. The power is negative during the braking process which shows the regeneration as shown in figure 24. The rise in SOC from 99.725% to 99.78% during braking in figure 25 also indicates regeneration.

The power analysis in the figure 26 shows that the mechanical power that converted to electrical power and finally stored in the battery is balanced with a slight difference that indicates losses in each power.

From all the above battery related graphs it can be seen that the graph during deceleration is not a constant graph. The battery current, battery voltage, battery power graphs decelerates their values at low speed. It can be seen that when deceleration starts a large amount of energy was regenerated at higher speed which shows that regenerative braking performance decreases at low speeds.

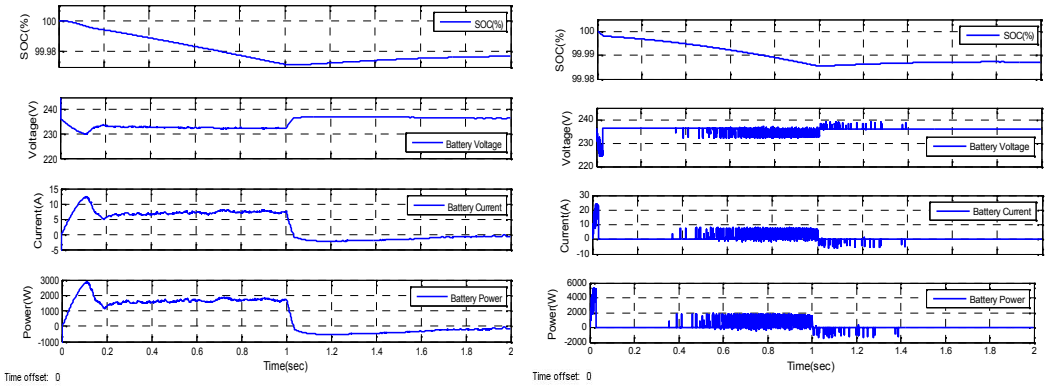

(a) (b)

Figure 27(a) overall regenerative braking performance using battery with bidirectional dc/dc converter, (b) overall regenerative braking performance using battery without bidirectional dc/dc converter

From figure 27 it can be seen that the regenerative braking with a bidirectional dc/dc converter has a better performance than without dc/dc converter. The battery current, voltage and power values fluctuate during regenerative braking, due to uncontrolled dc bus voltage for system without a bidirectional dc/dc converter.

Experimental Results

During Experimentation using C2000 F28035 kit,

The speed of an induction motor with different deceleration rate has been analyzed. The speed graph with 0.3pu, 0.2pu, 0.1pu and 0pu and their related torque controlling current component (i_q) and dc bus voltage (voltage across capacitor bank) are shown from fig 28 to 31.

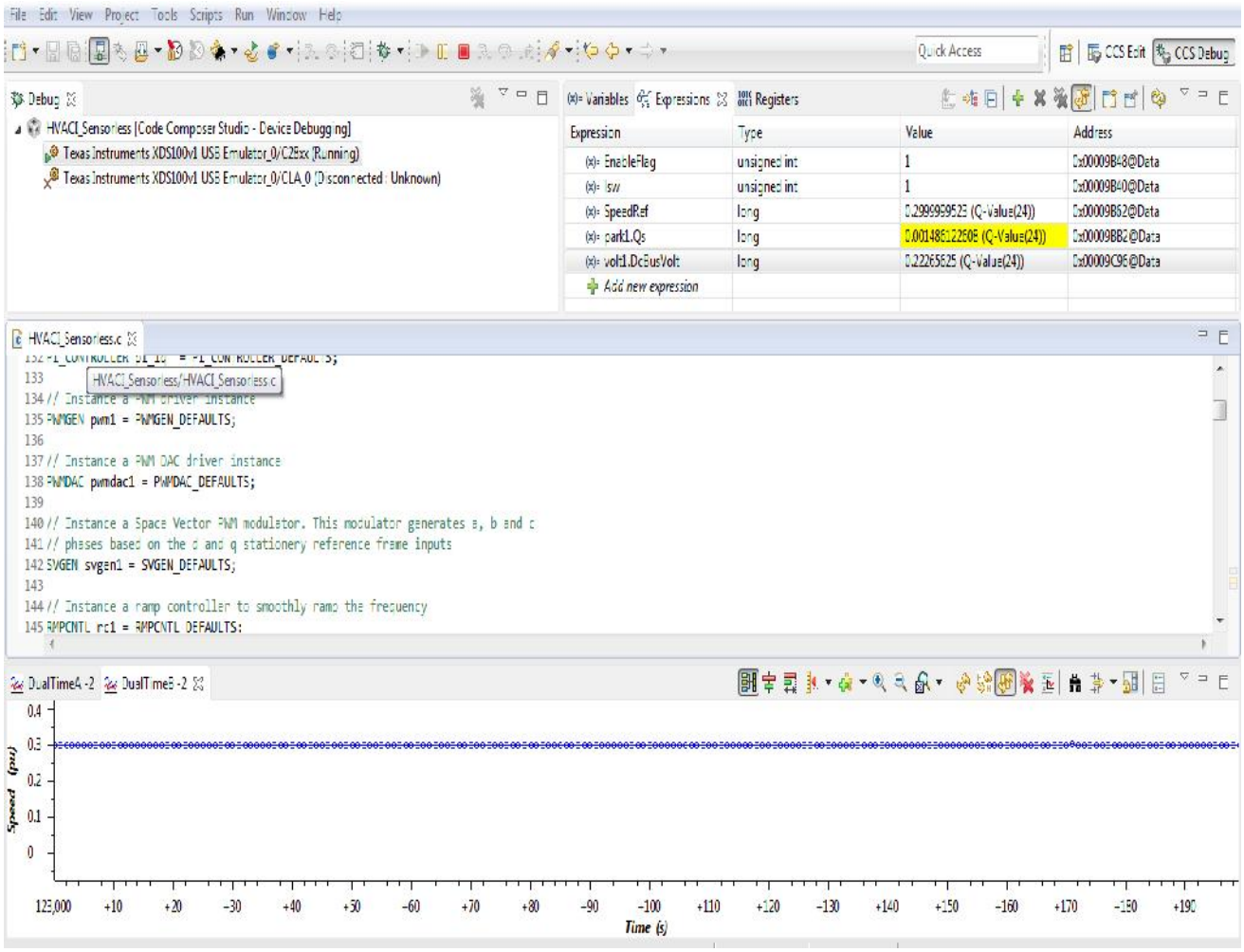

Figure28. Speed of IM at 0.3 pu

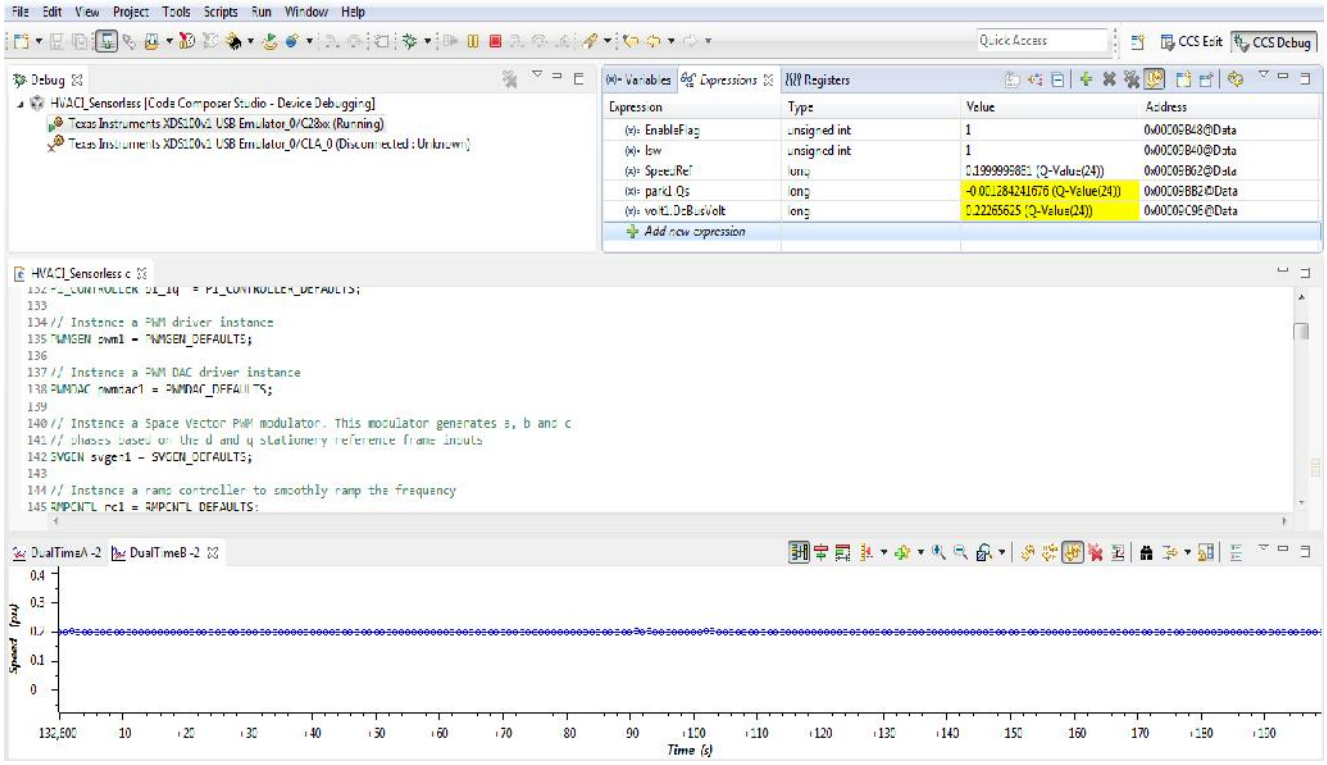

Figure 29Speed of IM decelerating to 0.2 pu

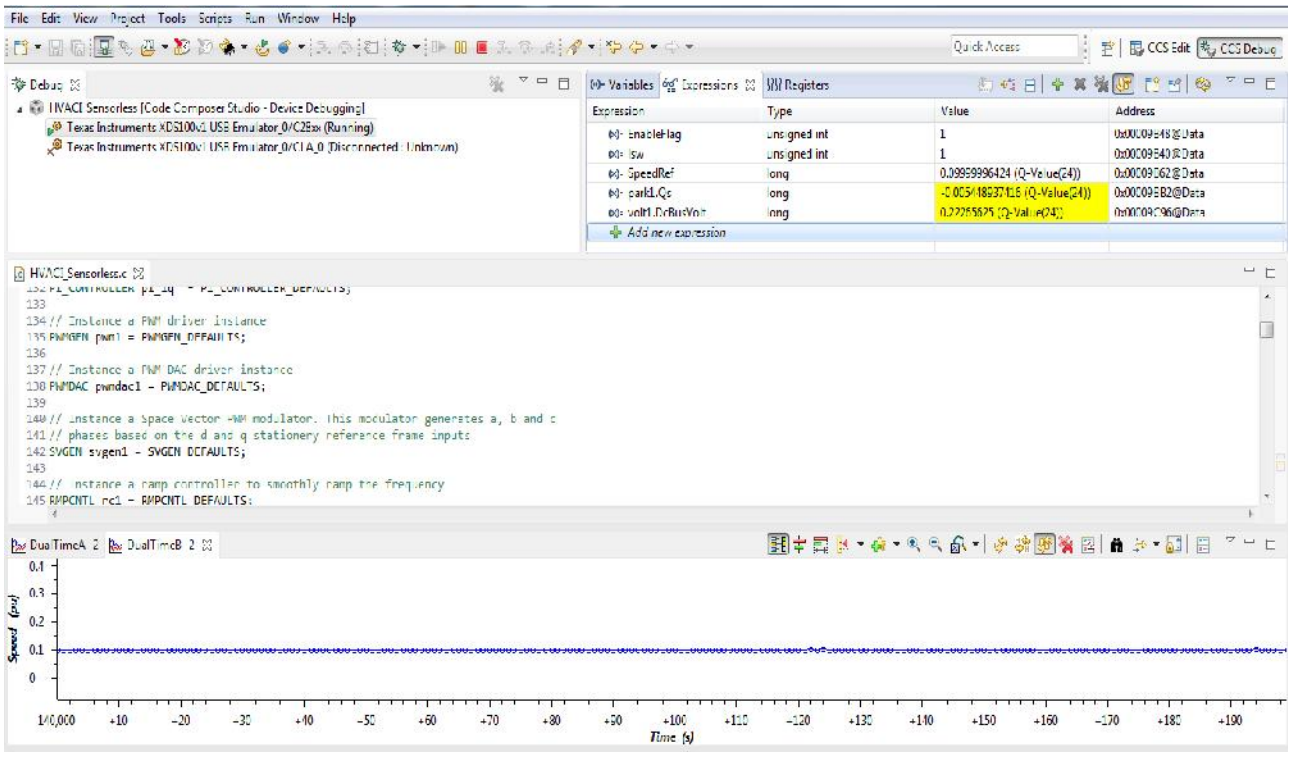

Figure30. Speed of IM decelerating to 0.1 pu

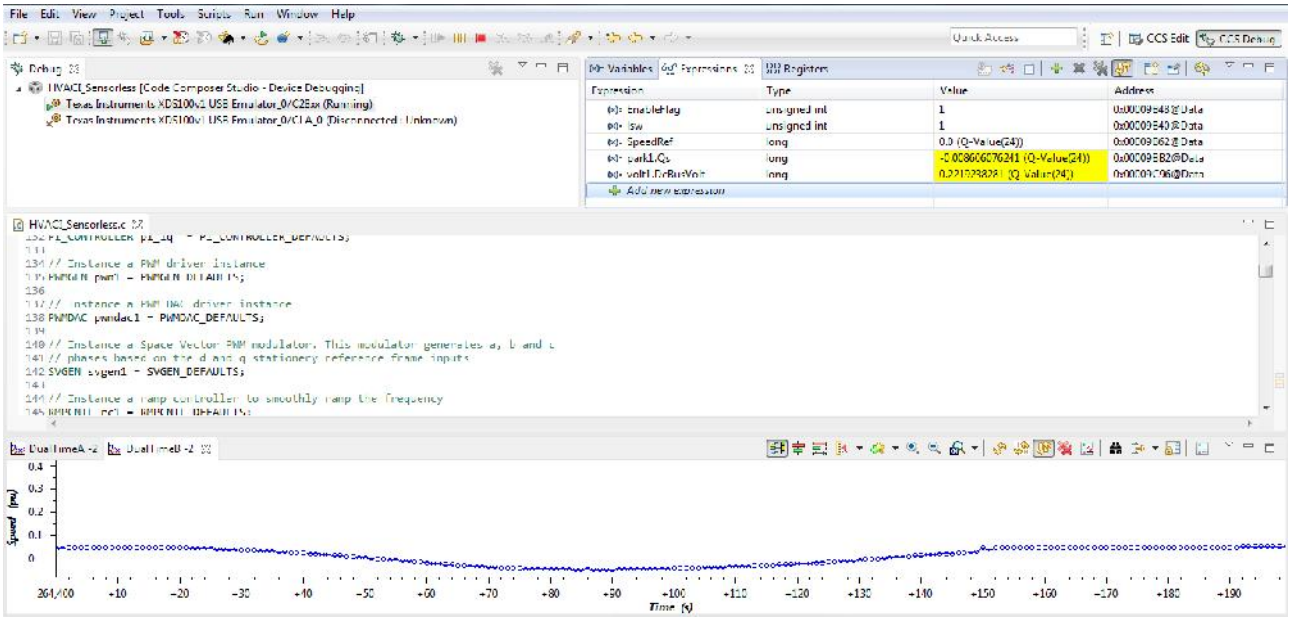

Figure31.Speed of IM decelerating to zero

From the above figures the overall system has a good speed performance at higher speed than lower. At lower speeds the speed estimator performance decreases. This is due to the open loop speed estimation technique used in this thesis. In figure 31 it is seen that the speed fluctuates at zero speed. This is due to the system is based on rotor flux.

The variation of torque controlling current component i_q('Park1.Qs' in the code) with respect to the speed of IM at different deceleration rates can be seen in the above figures.

From the above four figures it can be seen the value $i_q$become negative when the motor is decelerating. This indicates the motor is in regenerative braking mode.

It can be also seen that with decreasing motor speed, the values ofi_q increases in the negative direction. This also shows that the torque also increases in the negative direction which indicates a large braking torque is needed for full brake (zero speed). The dc bus voltage (which is around 0.2226 pu) shown in the figures (28-31)do not vary during deceleration of the motor due to the small value of inertia of the motor.

But, connecting additional disk to the motor increases the inertia of the motor and energy regeneration was observed.

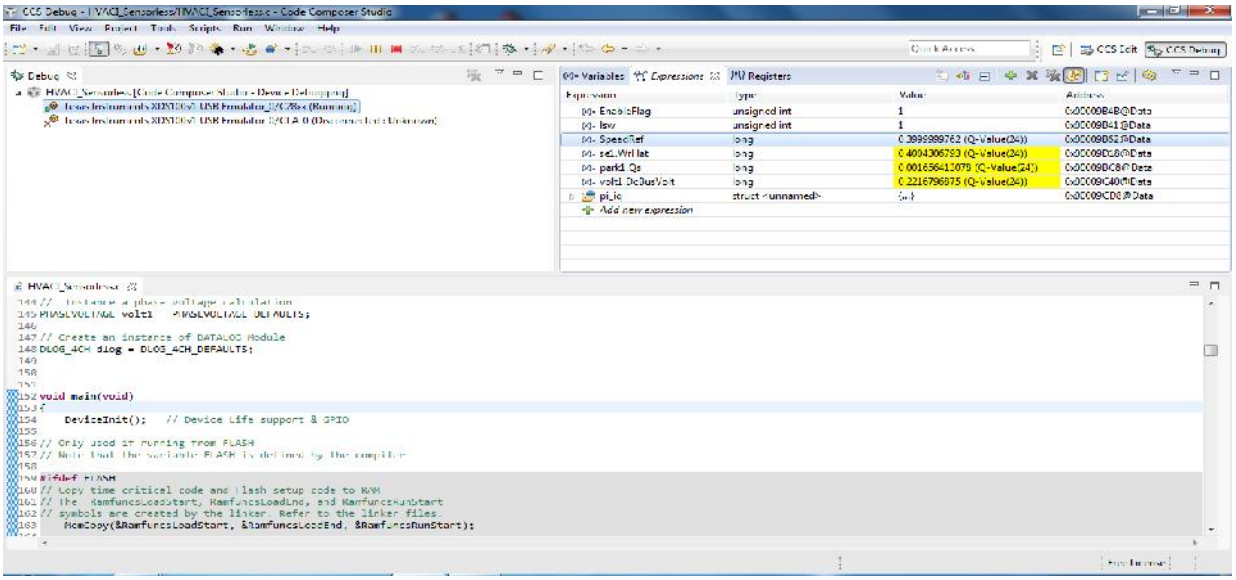

Figure 32: Speed of IM at 0.4 pu

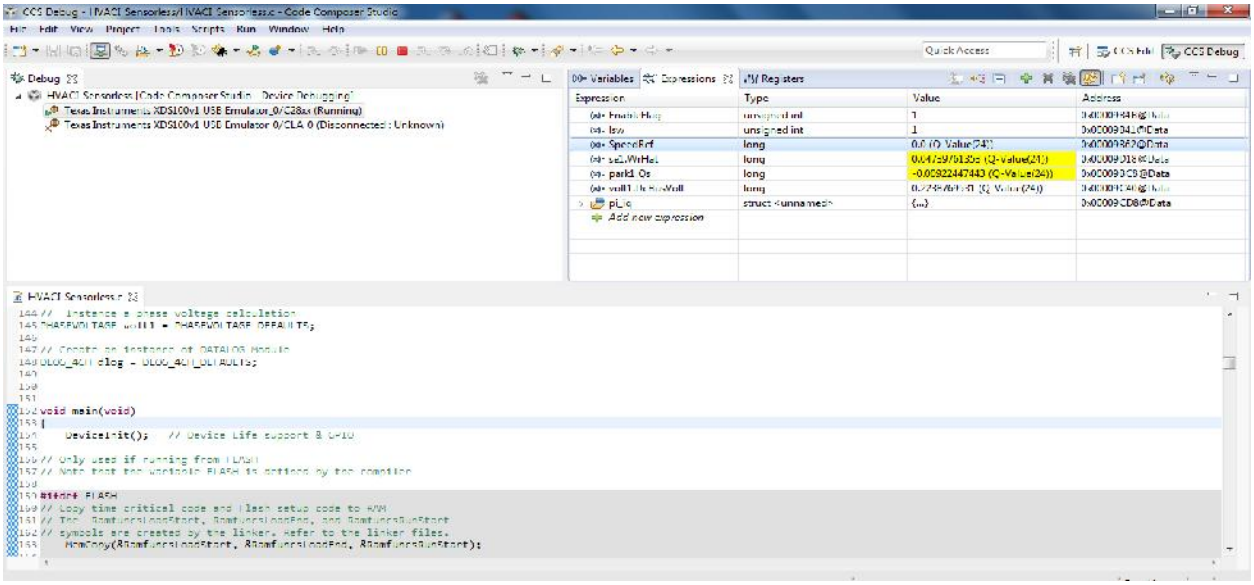

Figure 33: Speed of IM decelerates to 0 pu

Figure 32 &33 show that when the speed of the motor decelerates from 0.4 pu to 0 pu, the dc bus voltage shows a slight difference from 0.221679 pu to 0.223877 pu. Converting the per unit values to volt, it varies from 52.3384 to 52.857336 volt. This indicates that with an addition of a small disk to increase inertia of the motor, about 0.52 volt increase in the dc bus voltage was shown.

Another braking experimental analysis has also been performed on the motor by disconnecting the motor from the source and by giving Commanded braking torque that brake the motor through speed controller (by decelerating the motor) to observe the time it takes to decelerate. From these two experiments the time needed for full brake is analyzed. But since this thesis uses rotor flux based speed estimation which have a very low performance at low speeds, in this experiment the deceleration of the motor is considered below 10% of rated speed (not at zero speed). The time that takes for the motor to stop during regenerative braking from the experimentation is summarized in the table below.

Table5: Time data in braking IM

Experiments		Time takes to brake IM
1	By disconnecting the motor from the supply power	3.37 Seconds
2	By giving commanded braking torque through speed controller	2.35 Seconds

Using this two data the following graph is constructed below

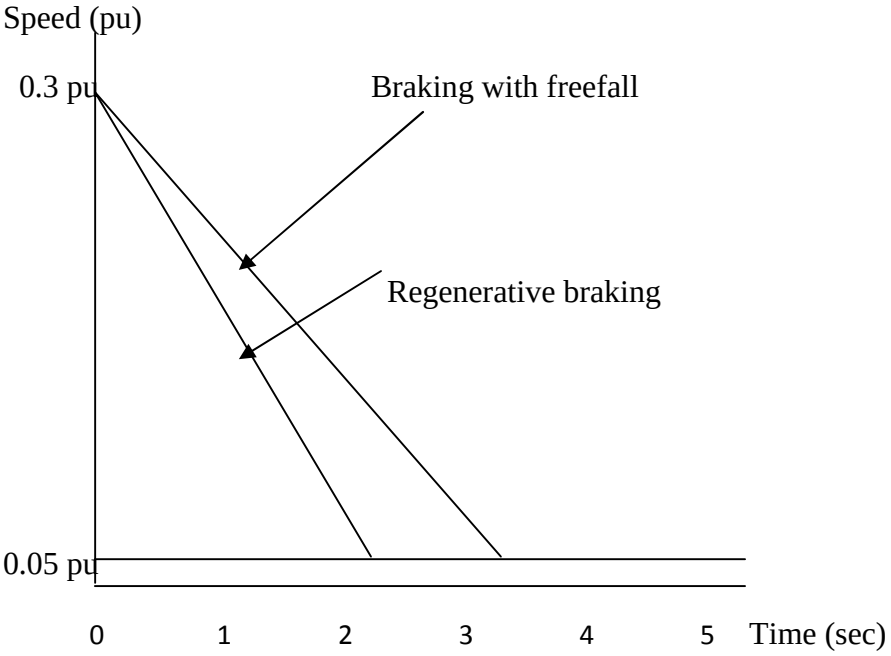

Figure 34 Free fall brake and Regenerative braking Time Analysis

From figure 34 one can see that the time it takes to brake IM using freefall is longer than using regenerative braking.

Chapter Five
Conclusion and Future Work Recommendation

5.1 Conclusion

The use of regenerative braking system instead of mechanical braking will save a great deal of energy. The regenerative braking system developed using converters and batteries have better efficiency than using only batteries.

In experimentation energy saving (around 0.5 volt variation)was also observed by increasing the inertia of the motor with an addition of extra disk since the kit can handle small motors (motor with small inertia).

In this proposed method, during regenerative braking power is back to the source in this case, the battery, which indicates energy has been saved.

5.2 Future Work Recommendation

The work is focused here on battery, converter and IM. But a simulation study can be performed using supper capacitors instead of batteries since super capacitor models are so easy than battery models. The experiment done on C2000 F28035 kit shows that only using its components a very small amount of energy can be saved during regenerative braking but adding additional converter circuits or by replacing the kit with F28035 microcontroller by a kit with F28069 microcontroller it may be possible to regenerate more energy in future.

References

[1] Dr.SJCLEGG, “A Review of Regenerative Braking System”, University of LEEDS, Institute of Transport Studies, ITS Working Paper 471, April 1996

[2] NedMothan, “Advanced Electrical Drives- Analysis Control and Modeling using Simulink MNPERE”, 2002

[3] B.Srinu Nalk, “Comparison of Direct and Indirect Vector Control of Induction Motor”, International Journal of New Technologies in Science and Engineering, Vol.1, Issue1, Jan.2014

[4] Marko Hinkkonen, Jorma Loomi, “Braking Scheme for Vector Controlled Induction Motor Drive Equipped with Diode Rectifier without Braking Resistor”, IEEE Transaction on Industry Applications, Vol.42, No. 5, September/October 2006

[5] Sandeep Goyat, Rajesh Kr.Ahuja, ”Speed Control of Induction Motor using Vector Control or Field Oriented Control”, Journal of Advances in Engineering and Technology, Vol.4, Issue 1, July 2012, pp 475-482

[6] Mr.Sandeep N Panchal, Mr.Vishal S shelth and Mr.Akshay A Pandya, “Simulation Analysis of SVPWM Inverter Fed Induction Motor Drives”, International Journal of Emerging Trends in Electrical and Electronics, Vol.2, Issue 4, April 2013

[7] Yogesh Abhale, Prateek Nigam, “Review on Regenerative Braking Methodology in Electric Vehicle”, International Journal of Advanced Research in Electrical, Electronics and Instrumentation Engineering, Vol. 4, Issue 7 July 2015

[8] Pedro Nuno da Costa Neves and Joao L.Afonso, “Traction System for Electric Vehicles using A Variable Frequency Three Phase Induction Motor Drives with Regenerative Braking”, HSCI’ 2006- 3rd International Conference on Hands- on Science- Science Education and Sustainable Development, Braga, Portugal, 2006

[9] Farad Sangtarash, Vahid Esfahanian, Hassan Nehzati, Samaneh Haddadi, Meisam Amiri Bavanpour and Babak Haghpanch, “Effect of Different Regenerative Braking Strategies on Braking Performance and Fuel Economy in a Hybrid Electric Bus Employing CRUISE Vehicle Simulation”, University of Tehran, SAE International, 2008

[10] Andrea Caratti, Gabriele Catacchilo, Carlo Gambino and Narayan C.Kar, “Development of a Predictive Model for Regenerative Braking System”, IEEE, 2013

[11] B.M.Bird, MLEE and P.Mehta, “Regenerative Braking in Slip-Power-recovery System”, PROC.IEE, Vol.119, No.9, September 1972

[12] Li-giang Jin, Ying Zheng, Jian-hua Li and Yu-long Liu, “A study of novel regenerative braking system based on super capacitor for electric vehicle driven by in-wheel motors”, Research Article Advances in Mechanical Engineering, 2015

[13] BoLong, Shin Teak Lim, Ji Hyoung Ryu and Kil To chang, “Energy- Regenerative Braking Control of Electric Vehicles using Three-Phase Brushless Direct Current Motors”, www.mdpi.com/journal/energies, 2014

[14] Ranjan, “Regenerative Brake: To Harness the kinetic energy of Braking”, Journal of Emerging Technologies and Innovative Research, Vol.2, Issue 1, January 2015

[15] Robyns, B.Francois, B.Degobert, P.Hautier, J.P, “ Chapter 2:Vector Control of Induction Machines Desensitisation and Optimization Through Fuzzy Logic”,2012

[16] Kapil Gandhi, Saurabh Saxena and Maroof Ali, “Vector Control of 3-Phase Induction Motor”, MIT International Journal of Electrical and Instrumentation Engineering, Vol.3, No. 2, August 2013, pp 85-88

[17] Bose B.K.Modern Power Electronics and AC Drives, 4th Edition, 2004

[18] Shuhui Li and Baoke, “Study of Battery Modeling using Mathematical and Circuit Oriented Approaches”, IEE Power and Energy Society General Meeting, pp1-8, 24-29, July 2011

[19] C2000 Systems and Applications, Texas Instruments,Inc. , Digital Motor Control, Software library, 2012

[20] Do-Hyun Kim, Yoon-Seok Lee, Byung-Moon Han, Ju-Yong Kim and Woo-Kyu Chae, “Grid-tied Power Converter for Battery Energy Storage Composed of 2-stage DC-DC Converter”, J Electr Eng Technol, Vol. 8, http://dx.doi.org/10.5370/JEET.2013.8.6.742

[21] Ramisetty Anil, Katuri Saiklshore, “Fuzzy Control for A Bidirectional Dc-Dc Converter That InterfacesUltracapacitor Energy Storage To A Renewable Energy System”, International Journal Of Professional Engineering Studies, Volume IV, Issue3, NOV2014

[22] Bilal Akin, Manish Bhardwaj, “Sensorless Field Oriented Control of Induction Motors”, Texas Instruments Inc. C2000 Systems and Applications

[23] Nagulapati Kiran, K. Lavanya, K.Trinad Babu and M.Sudheer Kumar, “Comparative Analysis of Two level Sinusoidal PWM and Space Vector PWM Inverter fed three phase

Induction Motor", International Journal of Innovation and Scientific Research, Vol. 18. No.1 Sep.2015, pp192-205

[24] G.Celentano et al, "Regenerative and Plug braking Operations of inverter-fed asynchronous motors", IEE Proc: Electric power Applications, Vol.144, No 6, PP 453-455, Nov 1997

[25] M.Convino et al, "Analysis of braking operations in present day electrical drives with asynchronous motors", IEEE International Conference Reclaim Electrical machines and Drive, PP. MB3/1.1-MB3/1.3, 18-21, May 1997

[26] Beck et al "Plugging an Induction Motor", IEEE Trans. Industry and General Applications, Vol. IGA 6, No 1, PP 10-18, Jan 1970

[27] H.A.Halrik et al, "Proposed Scheme for plugging three phase induction motors", 15th IEEE Mediterranean Electro technical Conference MELECON, PP.1-5, 25-28 April 2010

[28] K.ZHANG.J.LI et al, "Electric Braking Performance Analysis of PMSM for Electric Vehicle Applications", International Conference on Electronic and Mechanical Engineering and Information Technology, 2011

Appendix

Calculation of Battery Parameters

The mathematical relationships that can be used to calculate the battery parameters like Battery Constant Voltage (Eo), Internal Resistance R, Polarization Constant (K), Exponential Zone Amplitude (A) and Exponential Zone Time Constant Inverse (B) from the given ratings of Battery Voltage (Vbatt) and Battery Capacity (Q) for the required voltages are given by Eqn. (1) to Eqn.(5) below.

$$E_{o(2)} = E_{o(1)} * \frac{V_{batt(2)}}{V_{batt(1)}} \quad (1)$$

$$R_{(2)} = R_{(1)} * \frac{V_{batt(2)}}{V_{batt(1)}} * \frac{Q_{(1)}}{Q_{(2)}} \quad (2)$$

$$K = K_{(1)} \frac{V_{batt(2)}}{V_{batt(1)}} * \frac{Q_{(1)}}{Q_{(2)}} \quad (3)$$

$$A_{(2)} = A_{(1)} * \frac{V_{batt(2)}}{V_{batt(1)}} \quad (4)$$

$$B_{(2)} = B_{(1)} * \frac{Q_{(1)}}{Q_{(2)}} \quad (5)$$

Therefore based on these mathematical relations the battery parameters of the new battery pack are resulted as follows:

E_o=213.6V

R=0.333Ω

K=0.233V/(Ah)

A=18.5 V

B=2.3077 (Ah^{-1})